BIOMIMETIC PEG HYDROGELS FOR EX VIVO EXPANSION AND IN SITU TRANSPLANTATION OF RETINAL PIGMENT EPITHELIAL CELLS

BY

CORINA E. WHITE

A dissertation submitted to the

School of Graduate Studies

Rutgers, The State University of New Jersey

In partial fulfillment of the requirements

For the degree of

Doctor of Philosophy

Graduate Program in Biomedical Engineering

Written under the direction of

Ronke M. Olabisi

And approved by

_____

_____

_____

_____

New Brunswick, New Jersey

October, 2017

ABSTRACT OF DISSERTATION

Biomimetic PEG Hydrogels for Ex Vivo Expansion and In Situ Transplantation of Retinal Pigment Epithelial Cells

By CORINA WHITE

Dissertation Director:

Ronke M. Olabisi

In several retinal degenerative disease pathologies, the retinal pigment epithelium (RPE) cell monolayer becomes dysfunctional. This monolayer, along with the underlying Bruch's membrane, creates a selective barrier for transport into and out of the retina, as well as supports neural retinal cells through the secretion of several key proteins. One such disease in which this dysfunction occurs is dry age-related macular degeneration (AMD). AMD is the leading cause of blindness in developed countries. Currently no treatment exists for dry AMD. Previous studies in animal models using a tissue engineering approach of implanting cells on scaffolds, show promise for the treatment of dry AMD. However, this approach is not without challenges. Two major challenges that must be addressed are RPE cell migration and dedifferentiation and inflammatory response to transplantation.

Design and optimization of scaffold cues for the purpose of RPE transplantation remain relatively unexplored, specifically the mechanical

properties of the scaffolds. The first aim of this work seeks to isolate the effects of scaffold modulus on RPE cells grown on these scaffolds. This was accomplished through the use of a synthetic polymer scaffold and a short cell adhesion peptide sequence. The results of this study indicated significant differences between cells on different substrate moduli in cell cytoskeleton structure, cellular activity, and expression of inflammatory markers. Further work in this dissertation sought to promote the mature phenotype of RPE cells grown on scaffolds through Activin A supplemented media, scaffold encapsulated Activin A, and covalent bonding of Activin A on the scaffold surface. It was hypothesized that the Activin A chemical cue would provide rescue effects for cells demonstrating dedifferentiated characteristics. The results revealed that for cells on low modulus scaffolds, the mechanical environment was the dominating cue and the Activin A was unable to rescue these cells. However, the Activin A was able to affect cells on high modulus scaffolds. This finding demonstrates that when cultured on scaffolds with an appropriate modulus, exogenous factors, such as Activin A, can affect cell expression, morphology, and activity, while the wrong scaffold modulus can have devastating effects on survival regardless of chemical stimulation. These findings have broad implications on the design and optimization of scaffolds for long-term successful RPE transplantation.

DEDICATIONS

To my loving and supportive mother and father, AnneMarie and Mark White – Thank you for celebrating my successes, helping me learn from my failures, and encouraging me every step of the way

To my siblings, Julie Wikman, Jonathan White, and Daniel White – Julie, thank you for being a model of strength and kindness; Jon & Dan, thank you for making me the competitive, driven person I am today

To Joseph McCarthy – Thank you for always believing in me more than I believe in myself and for making me smile every single day

ACKNOWLEDGEMENTS

This dissertation is the culmination of years of dedication and perseverance. Because of the nature of academic research, there were many failures along the way. However, my support network provided unwavering encouragement and help to move forward. Without this support, I would never have been able to complete this journey.

First and foremost, my appreciation goes out to my advisor, Dr. Ronke Olabisi. Thank you for allowing me the freedom to dream up and work on this project and thank you for your guidance along the way. My thanks also go out to my other committee members, Dr. David Shreiber, Dr. Li Cai, and Dr. Marco Zarbin. The input and advice provided by my committee throughout my years of work was invaluable.

In addition to my committee members, several other faculty and staff members guided me during my time at Rutgers. Without Dr. Yarmush's mentorship and encouragement to think outside the box, I would not be the scientist I am today. A huge amount of my gratitude is given to the Biomedical Engineering department staff, particularly Robin Yarborough and Larry Stromberg, who have answered countless questions from me and have always been extremely helpful. They truly keep the department running smoothly.

I am also grateful for my funding sources during the course of my graduate career. In particular, the NIH sponsored Rutgers Biotechnology Training Program and Department of Education's GAANN Personalized and Precision Medicine fellowship. Without this financial support, much of this work and travel to conferences would not be possible.

Starting as a PhD student in a new lab, trying to develop protocols and design experiments, is not an easy task. This would have been nearly impossible without the aid of other doctoral students. I'd like to particularly thank the members of the Freeman lab, Dr. Emmanuel Ekwueme, Dr. Brittany Taylor, Daniel Browe, for all the help in learning PCR and scaffold mechanical testing; members of the Yarmush lab, particularly Paulina Krzyzczyk, for help with ELISAs and fluorescent microscopy; and members of the Li Cai lab for all their help in isolating chick RPE cells. Beyond academic support, my fellow students provided me with friendship – the importance of which cannot be measured. My sincerest thanks go out to Dr. Ana Rodriguez, Dr. Laura Higgins, Dr. Michelle Sempkowski, Sally Stras, and Paulina Krzyszczyk. Without our daily lunches, nights out, and all the laughs we shared, this entire experience would have been an unexciting drudge.

Finally, this thesis would not have been accomplished without the support of my family, boyfriend, and friends. The love and appreciation I have

for my parents, siblings and their spouses, nieces and nephew is beyond words. A special thanks goes out to my brilliant, kind nephew Tommy, who never fails to make me smile. I also cannot overstate how grateful I am to Joseph McCarthy for his support. He provided me with unwavering confidence throughout this journey. When I was down, he built me back up and he never allowed me to doubt myself. This work truly would not have been completed without him. And lastly, to all of my incredible friends, especially Carla Tressler, thank you for allowing me to endlessly complain to you, for helping me keep things in perspective, and for the daily laughs and love.

PUBLICATIONS AND PRESENTATION

Several sections of this dissertation and related research have been published in peer-reviewed journals and/or presented at scientific conferences.

Peer- reviewed journal publications:

C White, T DiStefano, R Olabisi. The influence of substrate modulus on retinal pigment epithelial cells. *J Biomed Mater Res Part A.* 2017:105

CE White, R Olabisi. Scaffolds for retinal pigment epithelial cell transplantation in age-related macular degeneration. *J Tissue Eng*. 2017: 8

Conference presentations:

C White, R Olabisi, "The effects of mechanical chemical scaffold surface cues on retinal pigment epithelial cells," World Biomaterials Congress, Montreal Canada (2016)

C White, R Olabisi, "The effects of scaffold rigidity on retinal pigment epithelial cells," The Symposium on Biomaterials Science, Woodbridge NJ (2016)

C White, R Olabisi, "The effects of scaffold rigidity on retinal pigment epithelial inflammation and dedifferentiation," Rutgers Biotechnology Program Annual Symposium, Piscataway NJ (2016)

C White, R Olabisi, "The effects of scaffold rigidity on retinal pigment epithelial cells," Association for Research in Vision and Ophthalmology Annual Conference, Seattle WA (2016)

C White, R Olabisi, "The effects of scaffold mechanical cues on retinal pigment epithelial cells," 30th Annual Laboratory for Surface Modification & Institute for Advanced Materials, Devices, and Nanotechnology, Piscataway NJ (2016)

C White, R Olabisi, "Designing surface cues of a synthetic hydrogel scaffold for retinal pigment epithelium tissue engineering," Biomedical Engineering Society Annual Meeting, Tampa FL (2015)

C White, R Olabisi, "A synthetic hydrogel scaffold to mimic the Bruch's membrane for retinal tissue engineering," Society for Biomaterials Annual Meeting, Charlotte NC (2015)

C White, R Olabisi, "Poly(ethylene glycol) diacrylate scaffold mimics elasticity of native Bruch's membrane for retinal tissue engineering," Biomedical Engineering Society Annual Meeting, San Antonio TX (2014)

C White, R Olabisi, "Retinal tissue engineering using cell-responsive poly(ethylene glycol) diacrylate hydrogel scaffolds," Johnson & Johnson Engineering Showcase, New Brunswick NJ (2014)

TABLE OF CONTENTS

TABLE OF FIGURES

CHAPTER 1 : BACKGROUND AND INTRODUCTION

Sections of this chapter are reproduced from the following citation:

C White, R Olabisi. Scaffolds for retinal pigment epithelial cell transplantation in age-related macular degeneration. *J Tissue Eng*. 2017. Vol 8.

1.1 Retinal Physiology

The retina is a complex structure that sits in the posterior of the eye. This structure is responsible for the transduction of light signals into neural signals that then travel to the brain for interpretation as vision. In a simplistic model, the retina can be broken down into two major components: the neural retina and the blood retinal barrier (Figure 1.1). Briefly, the neural retina is comprised of photoreceptors and various neural cells including ganglia amacrine, horizontal, and bipolar cells. When light hits the eye, it is focused onto the retina, more specifically the central retina known as the macula. The light reacts with photopigment on photoreceptors, producing a neural signal and stimulating the other neural cell types that lead to the optic nerve and eventually the brain, where vision occurs. The blood retinal barrier consists of the retinal vascular endothelium and its associated tight junctions, creating the inner blood retinal barrier and the retinal pigment epithelium and its associated tight junctions, creating the outer blood retinal barrier. While the inner blood retinal barrier is

extremely important for maintaining a healthy retinal microenvironment, this remainder of the section will focus on the outer blood retinal barrier as it is most relevant to this work.

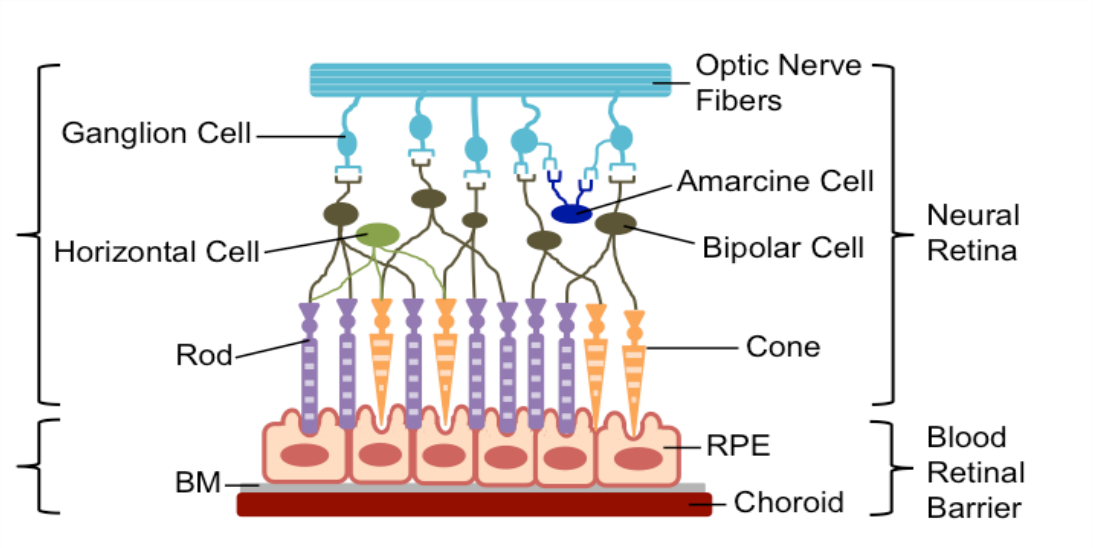

Figure 1.1: The structural organization of the retina. Diagram illustrating the distribution of retinal cells shows that photoreceptors interact directly with the apical side of the RPE cells. The RPE and other components of the blood retinal barrier maintain a healthy environment for the neural retina.

The major component of the outer blood retinal barrier (oBRB) is the retinal pigment epithelium (RPE). The RPE is a monolayer of pigmented cells that is characterized by its tight junctions. The RPE sits on top of a thin acellular membrane, the Bruch's membrane (BM). The BM is 2-4 μm thick and is

composed of collagen types I, III, IV, laminin, and elastin. Its main function is to provide structural support to both the RPE and the underlying vasculature as well.

The RPE has several key functions in maintaining a healthy retina and allowing the visual process to occur. [1] These functions include:

1. Light absorption: though a majority of the light that enters the retina is absorbed by the photopigment on photoreceptors, excess light is scattered. This function is important as it increases the visual acuity and prevents high-energy light photons from causing photo-oxidative damage.
2. Transport: with its tight junctions and high concentration of mitochondria per cell, the RPE selectively regulates transport as a barrier and through active transport mechanisms. This allows the RPE to provide nutrients to the neural retina and remove waste, metabolites, and water. The RPE is very much responsible for maintaining homeostasis in the retina.
3. Secretion of proteins and growth factors: in order to interact with both the photoreceptors and also with the cells of the choriocapillaris blood vessels, the RPE secretes many signaling molecules. These signaling molecules include many growth factors and inflammatory and anti-inflammatory cytokines. The secretion of proteins and growth factors is characteristically polarized, or directed either towards the neural retina or the underlying

vasculature. The RPE is also responsible for transport and regeneration of 11-cis retinal, a key molecule in the visual cycle.

4. Phagocytosis of photoreceptor outer segments: a major role of the RPE is to phagocytose the shed outer segments of photoreceptors. Photoreceptor outer segments, because they are constantly reacting to light stimuli, undergo high oxidative stress and are therefore replaced frequently. If this waste is not removed, photoreceptor death can occur.

1.2 Aging and age-related macular degeneration

There are several changes that occur to the RPE and BM as the body ages, many of which can drastically affect their ability to carry out their crucial functions to maintain a healthy retina. In the RPE there is an atrophy of its characteristic apical microvilli responsible for its close association with photoreceptors, and an accumulation of waste, including lipids and residual bodies (Figure 1.2). There is also an accumulation of deposits on or within the BM and formation of drusen, a yellow lipid-containing deposit, between the RPE and BM. In addition, the BM increases in thickness and stiffness due to increased levels of collagen cross-linking and there is a loss of hydraulic conductivity, affecting transport through the oBRB. [2]

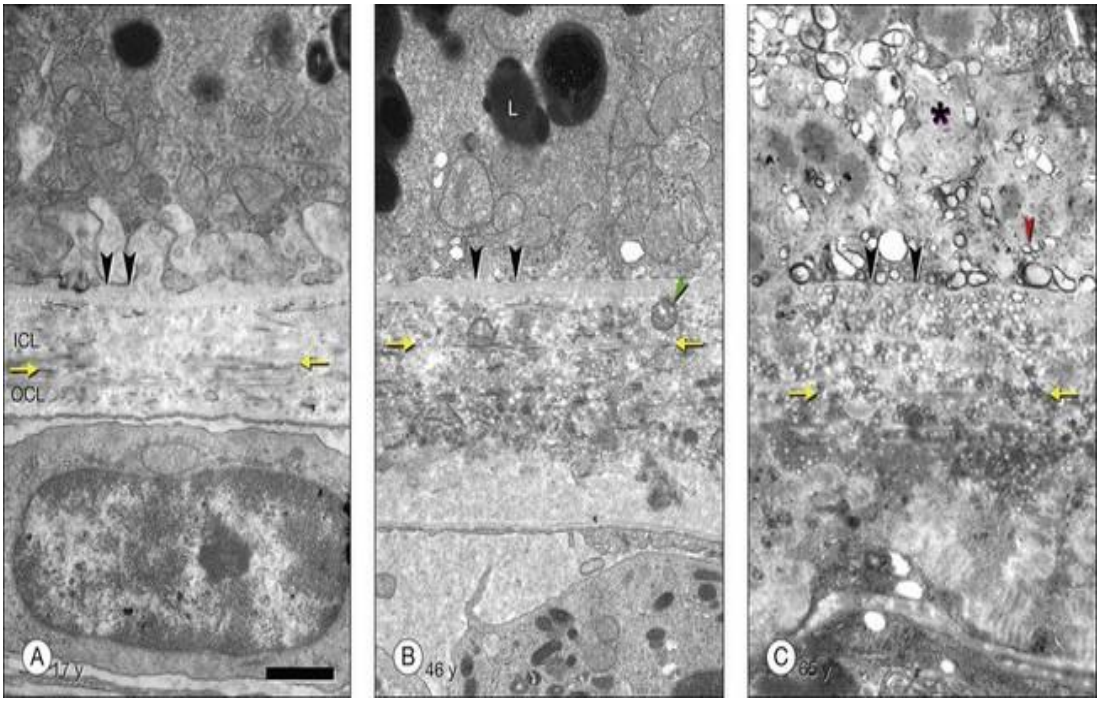

Figure 1.2: Macular Bruch's membrane throughout the lifespan. Retinal pigment epithelium (RPE) is at the top of all panels. RPE basal lamina (arrowheads) and elastic layer (EL, yellow arrows, discontinuous in macula) are shown. (A) 17 years: electron-dense amorphous debris and lipoproteins are absent. ICL, inner collagenous layer; OCL, outer collagenous layer. Bar = 1 μm. (B) 46 years: electron-dense amorphous debris and lipoproteins are present. Coated membrane-bound bodies (green arrow) contain lipoproteins. L, lipofuscin. (C) 65 years: electron-dense amorphous debris and lipoproteins are abundant. Membranous debris, also called lipoprotein-derived debris (red arrow), has electron-dense exteriors within basal laminar deposit (*). Within OCL, banded material is type VI collagen, often found in basal laminar deposit. Figure & caption from Curcio et al. [2]

In the retina, there is a symbiotic relationship between the photoreceptors, RPE, BM, and choriocapillaris. In the disease dry age-related macular degeneration (AMD), this relationship is lost. [3] Though the exact pathology of dry AMD is not fully elucidated, it appears that it is initiated by large confluent drusen formation and pigmentation changes to the RPE cells. Geographic atrophy, the death of an island-like area of the retina, including photoreceptors, is characteristic of AMD. As non-proliferative cells, photoreceptors cannot be replaced once they die. These islands of cell death lead to patches or black spots in AMD patients' vision and can drastically decrease their vision and quality of life (Figure 1.3).

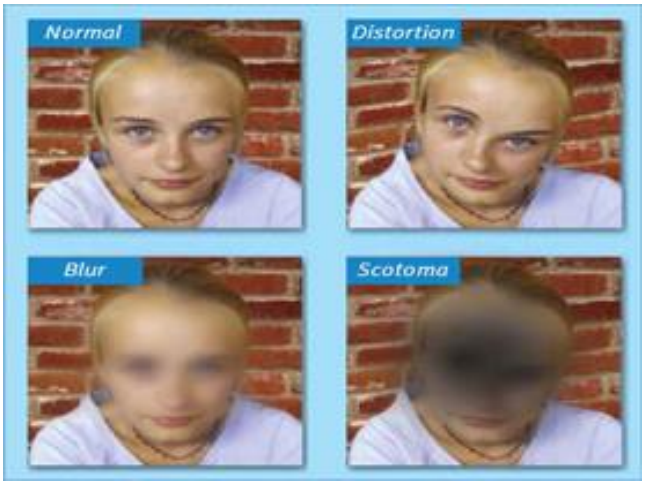

Figure 1.3: The progression of vision loss during dry AMD. Vision loss is generally slow during this disease, progressing from distorted vision to blur to scotoma, a blind spot of central vision. Figure from Retina Institute of the Carolinas & Macular Degeneration Center. [4]

1.3 Free Cell Therapy

Despite being one of the most commonly diagnosed diseases by retinal specialist and the leading cause of blindness among people over the age of 50, there is currently no treatment for dry AMD. [5, 6] However, for decades the therapeutic effects of transplanted RPE cells in delaying photoreceptor degeneration have been demonstrated in animal models.

In 2001, Lund et al. showed significant rescue of visual function using a spontaneously derived cell line (ARPE19) and an extensively characterized genetically engineered human RPE cell line (h1RPE7) as assessed by behavioral or physiological techniques in the Royal College of Surgeons (RCS) rat model that demonstrates retinal degeneration due to the MERTK gene mutation. [7] These positive results were demonstrated through 20 weeks, or 140 days post-transplantation. In addition to this study, several other publications have shown similar findings. [8-14] Wang et al. transplanted ARPE19 cells in the same model and demonstrated the ability of implanted cells to delay inner retinal degeneration. [15] In the same study ARPE19 cells were also used to preserve cortical visual function in RCS rats. More recently, researchers have turned to embryonic stem cell (ESC)-derived RPE cells. Lu et al. implanted ESC-derived RPE in RCS rats. [16] The cells were able to sustain visual function and photoreceptor integrity in a dose dependent fashion. This long-term study

demonstrated much of the same rescue as the previous studies and additionally, due to its later time points, revealed that the initial rescue began decreasing after post-transplantation day 90 (Figure 1.4). This reduced efficacy could be due to the injected ESC-derived RPE cells not interacting with the BM and thereby not forming a functional monolayer. The injected cells were observed above and adjacent to the native diseased RPE rather than penetrating and repairing the diseased RPE.

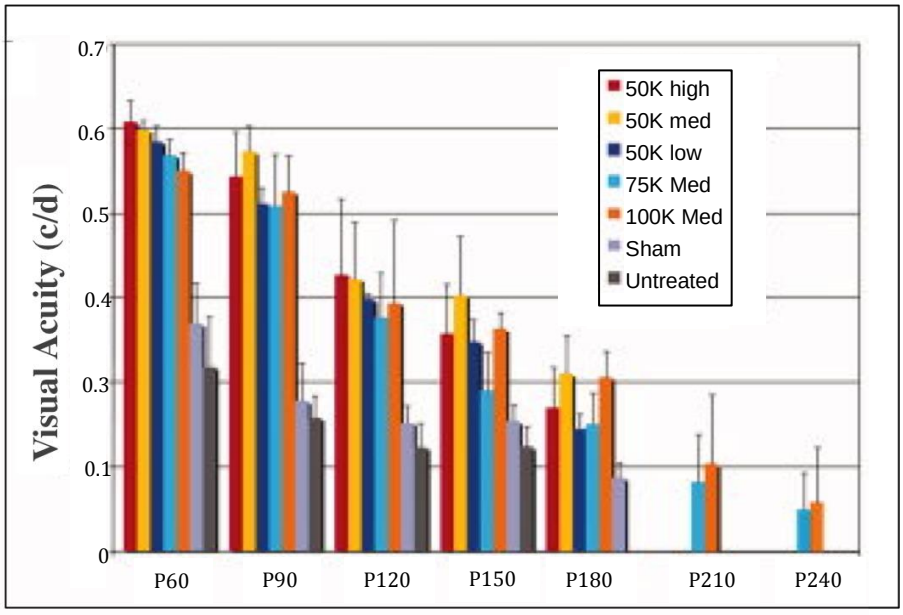

Figure 1.4: Batch and longevity of effect of subretinally injected human embryonic stem cell-derived RPE as measured by visual acuity. Rescue of visual function decreases after day 90 and by day 240 only the high dose groups still have low levels of visual acuity. Figure adapted from Lu et al. [16]

Beyond animal models, this approach has been taken to clinical trials for patients who have AMD or Stargardt's macular dystrophy, an inherited disorder that causes progressive damage to the retina much like AMD but in juvenile patients. [17] Though the results from the two Phase 1/2 clinical studies are preliminary, there was no evidence of adverse proliferation, rejection, or safety issues related to the transplanted cells. In addition, visual acuity improved in the treated eyes following the 22-month median follow up on the 18 eyes (9 Stargardt's macular dystrophy, 9 AMD). However, in these studies, the cells were purposefully transplanted in an area peripheral to the degenerating area. This approach uses the transplanted cells to rescue the degenerating cells through the release of neurotrophic factors. The exogenous cells were not forming the monolayer architecture or re-establishing the selective transport properties of the oBRB. This approach does show a benefit of implanting cells, but it does not address the primary insult of AMD, which is altered properties of the oBRB. The diseased-state RPE and BM properties must be addressed in order to promote an efficacious therapy in the long term.

1.4 Tissue Engineering Approach

The two main properties altered during retinal degeneration are the mechanical and transport properties of the BM. In the diseased state, the RPE monolayer is disrupted causing compromised cell-cell junctions, as well as altering cell expression patterns and function on an individual cell basis. In addition, the BM displays a higher level of collagen cross-linking and higher lipid and membrane-coated body content. An optimized tissue engineered scaffold seeded with a mature RPE monolayer can mimic a healthy BM state and address the aforementioned issues associated with retinal degeneration.

Such is the rationale and motivation in exploring scaffolds for RPE cell transplantation. The general consensus is that the ideal scaffold will meet the following requirements, it will [18-20]:

1. Be biocompatible and not induce inflammation,
2. Promote and maintain long-term healthy RPE phenotype,
3. Mimic healthy BM properties,
4. Be capable of being fabricated in optimal dimensions (5-90 μm), and
5. Be mechanically robust enough to withstand manipulation during implantation.

1.4.1 Natural Materials

Bruch's Membrane & Other Naturally Occurring Membranes

As with most transplants, one of the first options investigated for RPE transplantation was its native basement membrane, an autologous (e.g., translocated explant) BM. However, the aforementioned age-related changes in the BM present a hurdle for their use.

A unique approach to modifying BM explants involved first seeding corneal endothelial cells on a BM explant, allowing the seeded cells to deposit an extracellular matrix (ECM), removing the corneal cells, and then seeding RPE cells on the deposited ECM. [21] This cell-deposited matrix led to significant RPE nuclear density when seeded on aged sub-macular BM compared to untreated age-matched BM controls. In addition to BM explants, anterior lens capsules as scaffolds for RPE cells have been investigated. [22-25] This elastic membrane sits at the back of the lens anterior to the vitreous humor. Similar to the BM, it supports a monolayer of epithelial cells. When compared to synthetic polymer hydrogels, porcine anterior lens capsules supported higher cell density and viability than the hydrogel scaffolds. [25] Several other naturally occurring membranes have been investigated for their potential as RPE cell scaffolds, including human amniotic membrane, Descemet's membrane, and the inner

limiting membrane of the retina and all demonstrated the ability to support characteristic RPE morphology and expression in seeded RPE cells. [26-32]

Because AMD presents with high levels of degeneration in the macula that decreases towards the periphery, translocation of a full thickness choroid-BM-RPE complex has been attempted. This has mainly been performed in patients with the exudative, wet form of AMD but has also been attempted with dry AMD. The translocated grafts show revascularization and delayed degeneration, however surgical complications remain high and visual improvement has been limited. [33-35] In a long-term study by Zeeburg et al., one hundred thirty-three eyes with exudative AMD underwent a graft of the peripheral RPE-choroid complex. Prior to surgery, the average best corrected visual acuity (BCVA) was 20/250. At four years post-surgery, 15% of the eyes had BCVA worse than 20/200 and 5% had BCVA worse than or equal to 20/40. [36] Although the improvement in some participants' visual acuity is noteworthy, it is important to look at the bulk of the data which indicates that a vast majority, or 85%, of treated eyes were measured with BCVAs worse than 20/200, which is the cut-off for being characterized as legally blind. Obviously, there is still much progress to be made.

Using natural membranes has its benefits, such as containing the proper native ultrastructure and biochemical cues. However, donor variability and limited material availability motivate the use of non-membranous polymer

materials, both natural and synthetic, that can be fabricated into the desired dimensions.

1.4.2 Natural Polymer Scaffolds

Natural polymers are an attractive option for a number tissue engineering scaffolds. Because the BM consists of various types of collagens, collagen is the most studied natural polymer for BM scaffolds. Collagen shows great promise as a scaffold for many reasons, including its lending itself to a variety of fabrication techniques. As previously mentioned, the ideal scaffold will have similar dimensions to the natural BM, ideally less than 10 μm. In 2007, Lu et al. used thin film collagen scaffolds for the culture of RPE cells. These thin films had a thickness of 2.4 ± 0.2 μm and were able to maintain both cell viability and characteristic cell morphology. [37] Warnke et al. compared thin films to electrospun nanofiber collagen scaffolds and on these nanofiber scaffolds demonstrated better morphology of RPE cells, including more defined apical microvilli, a strong indicator of the health of RPE cells. [38]

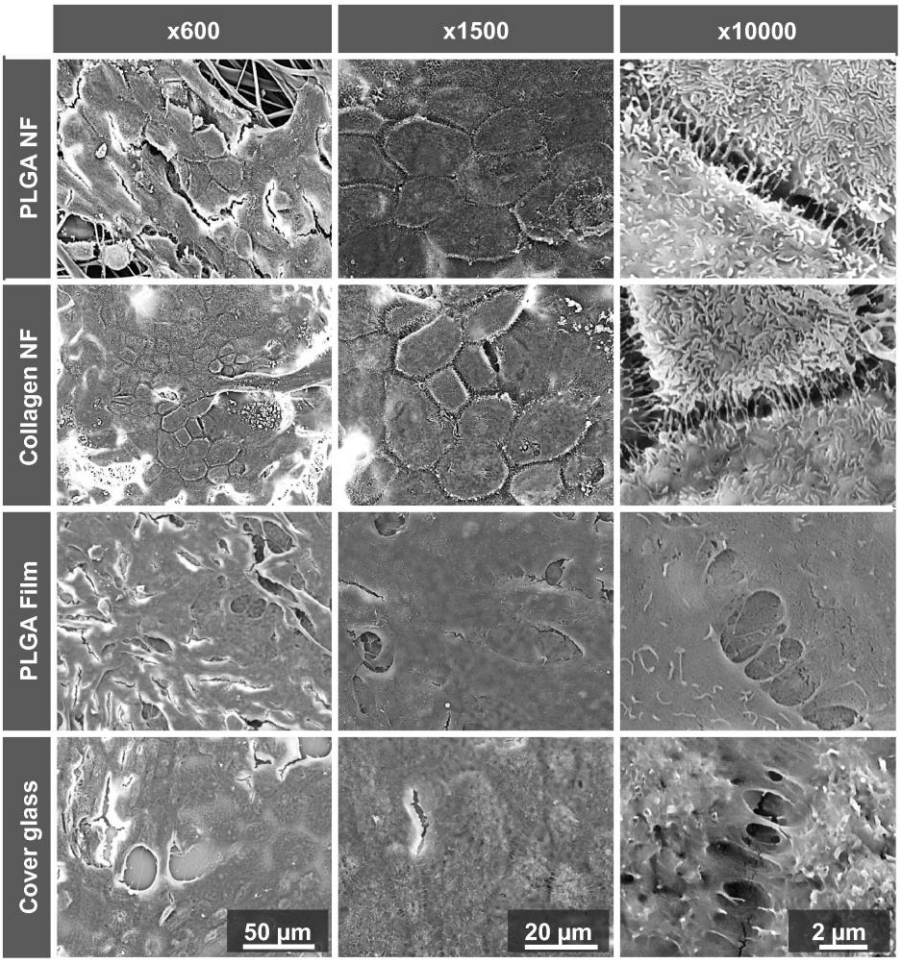

Figure 1.5: SEM images of RPE cells on PLGA and collagen nanofibrillar membranes (NF), PLGA films and cover glass after 11 days. The RPE cells on NF membranes form an *in vivo*-like monolayer. Cells on NF membranes also demonstrate long, sheet-like microvilli while cells on flat surfaces appear less organized. Figure reprinted from Warnke et al. [38]

Interestingly, these collagen nanofiber scaffolds did not show significant differences compared to poly(lactic-co-glycolic acid) (PLGA) nanofiber scaffolds. [38] Although collagen is the most highly investigated scaffold material, human cryoprecipitate, gelatin, and crosslinked fibrinogen scaffolds have also been investigated with some promising results. [39-42] Cryoprecipitate offers a unique benefit in that it can be harvested from the patient's own blood, removing the risk of rejection. Farrokh-Siar et al. seeded cryoprecipitate membranes with fetal RPE sheets. [39] The sheets maintained their morphology and proliferated during culture. Both fibrinogen and gelatin were evaluated *in vivo* in rabbits and pigs, respectively. The crosslinked fibrinogen was prepared into microspheres and seeded with human fetal RPE cells, which survived up to one month. However, there was evidence of a mild local inflammatory response. In the Del Priore study that used gelatin, there was a presence of macrophage or macrophage-like cells in the retina, as well as lymphatic cells within the lumen of the choriocapillaris blood vessels underlying the transplant site. [41] These indicators of immune response serve as a predictor of the death of the transplanted RPE cells. Reducing the expression of inflammatory cytokines and recruitment of immune cells should be considered during scaffold design. While these natural polymers have the benefits of biocompatibility and biochemical cues present in the natural extracellular environment, serious drawbacks such as issues with

product purity, disease transmission, immune response, and difficulty in functionalization or modification do arise.

1.4.3 Synthetic Polymer Scaffolds

There have been several synthetic polymers investigated for use as a BM scaffold including poly(L-lactic acid)(PLLA), poly(lactic-co-glycolic acid) (PLGA), PLLA-PLGA co-polymer systems, poly(caprolactone) (PCL), methacrylated hydrogels, and parylene-C. PLLA and PLGA scaffolds were among the first materials to be investigated for RPE cell delivery and have been investigated by many groups. [43-46] These scaffolds, mostly fabricated through solvent casting into thin films, have been seeded with D407 RPE cells, human fetal RPE cells, and porcine RPE cells. These scaffolds have repeatedly demonstrated the ability to support viable RPE cells with proper morphology and phenotype. [19, 43, 44, 46, 47] Porous PCL, fabricated using photolithography and ion etching to create a scaffold mold, demonstrated improved markers of maturity and function of seeded fetal human RPE cells compared to non-porous PCL and porous polyester transwells. [20] Singh et al. compared methacrylate/methacrylamide copolymer hydrogels directly to porcine lens and found each scaffold supported similar cellular densities for both

human and porcine RPE cells. [25] The cells also maintained their phenotype and formed monolayers on both materials.

The use of synthetic polymers allows for more control over scaffold parameters such as mechanical and transport properties and degradation characteristics. While degradation may be desirable, the ideal degradation rate has not yet been identified since it depends both on the ability of RPE cells to generate their own matrix and the state of the BM at the time of cell transplantation. Many synthetic materials have been investigated as scaffolds for RPE cell implantation, no single material has jumped to the forefront of the field since positive results such as high cell viability, characteristic expression, and cell markers can be obtained on several materials. Besides material selection itself, the scaffold design parameters such as scaffold thickness and transport properties, and the ability to promote cell adhesion, appear to be the most important factors in controlling RPE fate and scaffold success in animal studies.

One of the most promising synthetic polymer scaffolds reported is fabricated with soft lithography using parylene-C. [48] This sub-micron mesh scaffold, supported by a 6 μm frame, is designed to mimic BM transport properties and is able to support RPE cells *in vitro*. These scaffolds were seeded with RPE cells, then implanted into the subretinal space of athymic nude rats. When compared to scaffold-free cell suspensions, cells transplanted on parylene-

C scaffolds survived in greater numbers. However, infiltration of macrophages was observed to a higher extent when scaffolds were present. [48, 49] In addition to scaffold dimension and transport property design, scaffold surface modification, specifically by plasma treatment, has been investigated. Oxygen, air, and ammonia gas plasma treatments to increase scaffold hydrophilicity have all demonstrated a variety of positive effects in cells cultured on these scaffolds. For instance, oxygen plasma treated scaffolds investigated by Tezcaner et al. demonstrated that as the oxygen treatment level was increased, hydrophilicity also increased while surface roughness was decreased on the poly(hydroxybutyrate-co-hydroxyvalerate) thin film. [50] The oxygen treatment increased attachment and spreading of D407 RPE cells. However, this improvement was modest and not statistically significant. Williams et al. investigated commercially available polyurethanes treated with air plasma to increase their wettability of the substrate. [51] Prior to treatment, only a few ARPE-19 cells attached and remained aggregated. However, after treatment, cells grew into a monolayer with the characteristic cobblestone morphology. [51] ARPE-19 cells were also used by Krishna et al. on ammonia plasma treated expanded polytetrafluoroethylene scaffolds. [52] The ammonia treatment resulted in enhanced growth and monolayer formation with phagocytic ability, reducing the amount of lipid waste buildup in the retina.

1.5 Thesis Overview

The broad, long-term scope of this work is to design an optimized scaffold for the *in vitro* expansion of RPE cells on a scaffold and transplantation of the RPE-scaffold complex to re-establish the compromised blood retinal barrier in AMD. Within that larger goal, the focus of this dissertation is to (1) understand how the mechanical properties of the scaffold affect RPE cells cultured on them and (2) to determine if functionalization of the scaffold with relevant, well-characterized retinal signaling molecules enhances viability, cell adhesion, cell morphology, and expression of the RPE cells in culture.

Chapter 2 discusses the effects of modulus on RPE cells. Specifically, it details the fabrication methods and testing of hydrogels to determine the moduli. This work is followed by the culturing of RPE cells on the scaffolds of varied modulus. Throughout 14 days of culture, cell adhesion, cell metabolism, cytoskeleton morphology, and gene expression were studied.

Chapter 3 describes the addition of Activin A to this system in supplemented media, encapsulated in scaffolds, and covalent functionalization of the scaffold surface. Activin A, known to promote a mature, non-proliferative RPE phenotype was conjugated to the surface of the scaffolds. [53] Following seeding of RPE cells on the surface, the effects of this signaling molecule on the RPE adhesion, metabolism, cytoskeletal shape, and gene expression was analyzed.

Finally, chapter 4 of this dissertation summarizes the findings and discusses the significance of this work to the field of retinal tissue engineering. Furthermore, this chapter lays out the importance of optimizing additional design parameters in order for scaffolds to successfully translate into a long-term clinical treatment.

CHAPTER 2 : THE EFFECTS OF SCAFFOLD MODULUS ON RETINAL PIGMENT EPITHELIAL CELLS

Sections of this chapter are reproduced from the following citation:

C White, T DiStefano, R Olabisi, The influence of substrate modulus on retinal pigment epithelial cells.*J Biomed Mater Res Part A* 2017: 105A:1260-1266.

2.1 Introduction

Scaffold substrate modulus has been demonstrated to affect cell adhesion, migration, expression and function in a variety of cells. [55-57] However, in the majority of previously published scaffolds intended for RPE transplantation, scaffold modulus has largely been neglected as a design parameter. Substrate modulus is an especially important parameter for anchorage-dependent cells such as RPE cells. RPE cells' dependence on adhesion to a matrix is so great that once detached, they are known to initiate anoikis – cell death due to detachment. [58]

In a Science review, Discher et al. discuss the key roles adhesion complexes play in molecular pathways and in the cytoskeleton of many different cell types, including epithelial cells. [59] Pelham et al. performed one of the first studies investigating the effects of scaffold modulus and used epithelial cells and fibroblastic cells on polyacrylamide hydrogels of varying modulus. [60]

Compared with cells on stiff gels, those on softer, more compliant substrates showed reduced cell spreading, higher rates of motility, and more dynamic cell adhesions.

It has been established that RPE adhesion is altered on aged BM, which is known to have an altered modulus. [21,61] It is also known that during RPE dedifferentiation a change in the expression of several genes, especially genes associated with the cytoskeleton and cell adhesion such as cytokeratins, α-smooth muscle actin, and fibronectin, is observed. [62,63] Such RPE responses support the rationale that understanding how scaffold modulus affects RPE cells may lead to better scaffold design and improve the *in vivo* fate of seeded RPE cells.

In addition to previous research on scaffolds, extensive research has been done to understand RPE trans- or dedifferentiation. RPE cells are known to dedifferentiation into a fibroblastic- or macrophage-like phenotype. [64] The mechanisms of RPE dedifferentiation have also been somewhat elucidated while current work seeks to more fully understand this transition. SMAD3 has been implicated as a key player in dedifferentiation. [62] It has also been noted that alpha-smooth muscle actin (αSMA) expression changes, as does the arrangement of the actin cytoskeleton during RPE dedifferentiation. [65]

Towards that end, this chapter, investigates how changing the modulus of a synthetic scaffold affects seeded RPE cells. Poly(ethylene glycol) diacrylate (PEGDA) is a highly bio-inert synthetic polymer with tunable mechanical properties. [66] Often referred to as a "blank slate," the lack of any substantive biological cues in PEGDA hydrogels permits evaluating the effect of scaffold modulus on RPE cells without other confounding variables. By functionalizing PEGDA with the cell adhesion protein sequence, RGDS, it was possible to use PEGDA as a cell substrate and thus isolate and systematically study how the modulus of a scaffold affects the viability, cell adhesion, cytoskeleton morphology, metabolic activity, and gene expression of both an established RPE cell line, ARPE-19, and primary embryonic chick RPE cells.

2.2 Materials and Methods

All reagents were purchased from Sigma-Aldrich (Saint Louis, MO, USA) and all PEGDA was obtained from Laysan Bio, Inc (Arab, AL, USA) and used as obtained without further purification unless otherwise noted.

2.2.1 Scaffold Fabrication

Hydrogel scaffolds were prepared using a polymer solution containing one of four different molecular weight PEGDA (Laysan Bio, Inc., Arab, AL, USA)

in HEPES-buffered saline (10 mM N-[2-hydroxyethyl]piperazine-N0-[2-ethanesulfonic acid] and NaCl in ultra pure water), with 10 μL/mL photoinitiator solution (2,2-dimethoxy-2-phenyl-acetophenone 300 mg/mL in N-vinylpyrrolidone). The four molecular weights of PEGDA used were 3.4 kDa, 5 kDa, 10 kDa, and 20 kDa. The concentrations used for 10 kDa and 20 kDa PEGDA were 10% and 20% for each weight. The concentrations for 3.4 kDa and 5 kDA were 20% and 40%. Lower PEGDA concentrations are defined as 1x and the higher concentrations as 2x, summarized in Table 2.1. The scaffolds were fabricated using molds constructed of two 25 mm x 75 mm pre-cleaned glass microscope slides separated by a 500 μm thick Teflon spacer. The molds were disinfected with 70% ethanol and exposed to UV light (B-200SP UV lamp, UVP, 365 nm 10 mW^2/cm^2) for further sterilization for at least an hour prior to use. The prepolymer PEGDA solutions were injected into the molds through a 0.2 μm polyethersulfone syringe filter, then the molds were exposed to the UV light for 3 minutes. The prepolymer solution underwent free radical polymerization during the exposure (Figure 2.1). Following polymerization, rectangular-shaped hydrogel scaffolds were removed from the molds with tweezers and fully immersed in 5 mL phosphate buffered saline (PBS) within petri dishes and allowed to swell for 24 hours in a humidified incubator.

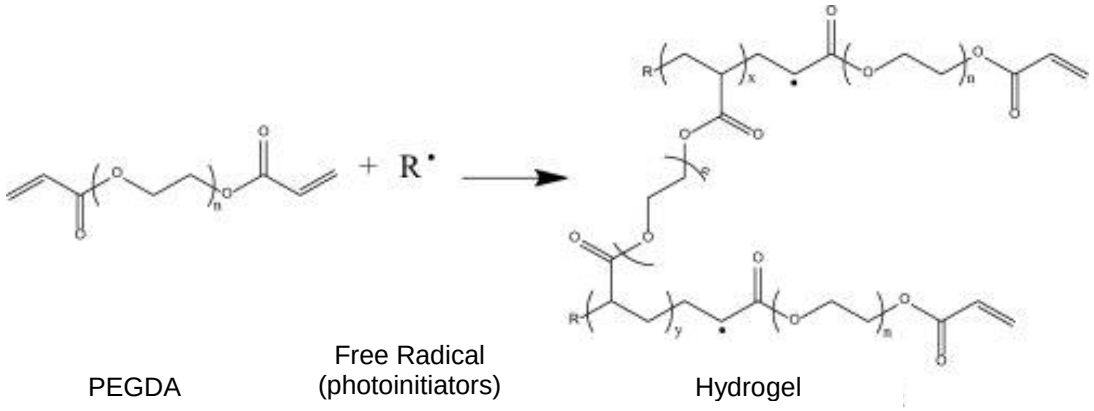

Figure 2.1: PEGDA free radical polymerization. Hydrophobic acrylate groups cluster in the aqueous PEGDA prepolymer solution. Exposing photoinitiators to light generates free radicals, which crosslinks the clustered acrylate groups. The reaction is terminated with the annihilation of the free radicals.

2.2.2 Characterization of Elastic Modulus

Young's moduli (E), or elastic modulus, of swelled scaffolds were determined by performing both tensile and compressive testing. Tensile testing was completed using a Bose Electroforce 3100 with a 1 Newton load cell. Hydrogel scaffolds were removed from PBS immediately prior to testing to maximize their hydration during testing. Testing lasted approximately 3 minutes for each scaffold, which was far less than the 20-30 minutes it takes for these scaffolds to dry. The hydrated hydrogels' thicknesses and the working distance between clamps were measured in mm using digital calipers. The average thicknesses of high and low modulus scaffolds were 0.61±0.03 mm and 0.58±0.05

mm, respectively. Though the differences were not statistically significant, the measured thicknesses were used to calculate the cross-sectional area of each hydrated hydrogel. The measured cross-sectional area values were in turn used to calculate the applied tensile stress from the force measurements returned by the Bose device. Following measurement, scaffolds were clamped at either end. Bose Electroforce flat knurled face tension grips were mounted vertically and the grips' inner faces were modified with duct tape to pad the surfaces. This prevented the sharp edges of the grips from pinching through the scaffolds. The scaffolds were tested in uniaxial strain applied at a rate of 6 mm/min. WinTest® 7 software was used for system control and force data acquisition. The data was collected and used to calculate the elastic modulus from the slope in the linear portion of the stress-strain curve (N= 40 total; n=5 for each molecular weight concentration).

Similarly, the scaffolds were tested in compression immediately after swelling. Compressive stress was applied using an Instron 5869 (Instron, USA) with a 50 kN load cell. A 1 mm/minute strain rate was applied to the scaffolds and they were tested to failure. The data was collected and, as for tensile testing, the elastic modulus was determined from the slope in the linear portion of the stress-strain curve. Representative raw data from both tension and compression testing can be seen in Figures 2.2A and 2.2B, respectively.

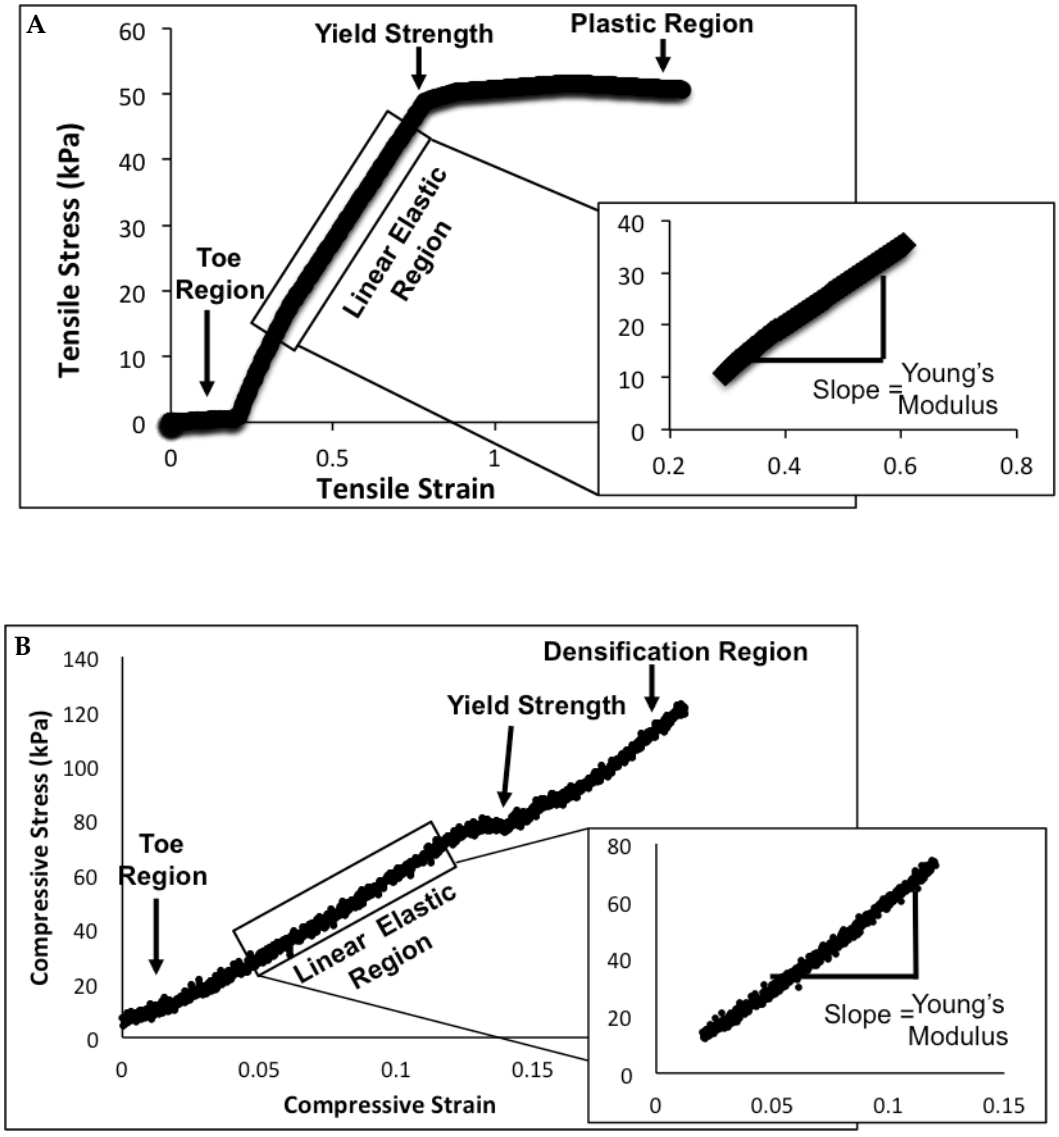

Figure 2.2: Raw data from testing hydrogels in both tension (A) and compression (B). In both conditions, by isolating the linear elastic region and determining the slope, the Young's Modulus was calculated.

The Young's Modulus (E) was then used to calculate the bulk modulus of the hydrogel using equation 1.

$$K = \frac{E}{3(1-2\upsilon)} \quad (1)$$

where the Poisson's ratio (ν) is equal to 0.45. [70]

2.2.3 Scaffold Fabrication & Glass Slide Functionalization

2.2.3.1 Synthesis of Acryl-PEG-RGDS

Heterobifunctionalized Acrylate-PEG-Succinimydal Valerate (ACRL-PEG-SVA; Laysan Bio, Inc., Arab, AL, USA) was reacted with RGDS (Tocris, Bristol, UK) in a 1:1.2 molar ratio at pH 8.0 under argon. The reaction mixture was placed on a rocker on its highest tilt and speed overnight in a 4°C cold room. Following overnight reaction, the solution was then dialyzed against 4 liters of ultra pure water in a 1000 MWCO cellulose membrane (Spectrum Labs, Rancho Dominguez, CA, USA), lyophilized, and stored at -20°C.

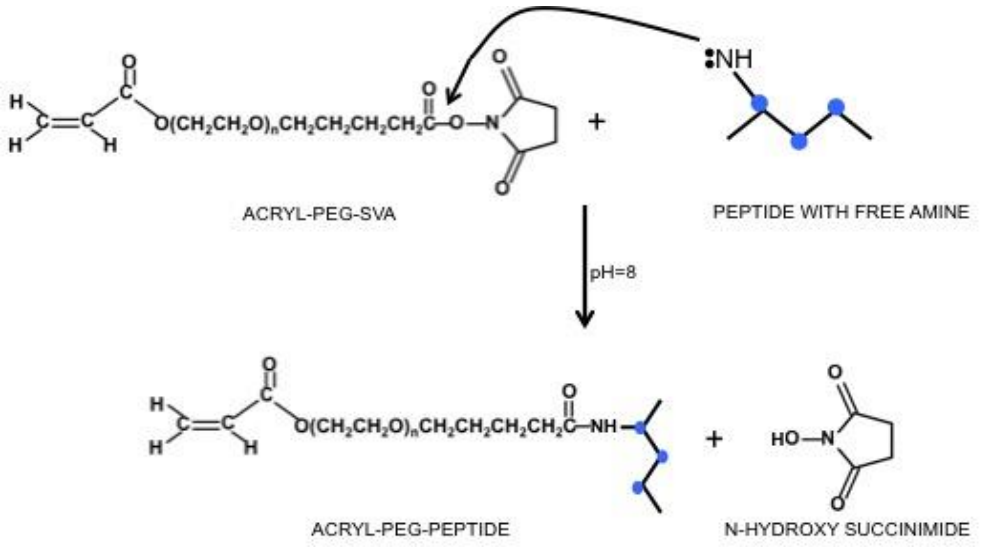

Figure 2.3: Reaction mechanism of functionalizing heterobifunctionalized PEG with a peptide. ACRL-PEG-SVA contains an active ester at the SVA which reacts with the free amines at the N-terminus, in lysine, or in arginine within peptides or proteins. When run at pH 8, the reaction results in an amide bond between the active ester and peptide and a by-product of n-hydroxy succinimide.

2.2.3.2 Confirmation of RGDS Conjugation

Ninhydrin assays were performed to measure the amount of free RGDS following the conjugation reaction with ACRL-PEG-SVA. Ninhydrin reacts with free amines and produces a purple colored product. This colorimetric assay

permits the measurement of unconjugated RGDS via reaction with free amines on the arginine. Briefly, prior to dialyzing the reaction solution, a 250 μL sample was lyophilized and reconstituted in PBS (100 μL). This reconstituted solution was next added to sodium citrate buffer (100 μL) and 2% ninhydrin solution (200 μL) in an Eppendorf low protein binding tube. This was then placed in a boiling water bath for 15 minutes. Absorbance of the solution was read on a Beckman DTX 880 Multimode Detector at 570 nm. A standard curve was produced using known concentrations of RGDS.

2.2.3.3 Scaffold Preparation for Cell Culture

Peptide-modified scaffolds were fabricated using the scaffold fabrication process described above with the addition of 10 mM ACRL-PEG-RGDS to the polymer solution. Scaffolds were then swelled in complete culture media (described below) for 24 hours, changing the media regularly for the first 8 hours to allow unconjugated peptide to diffuse out. For cell culture, a low modulus (E = 60 kPa) scaffold made with 0.1 g/mL 20 kDa PEGDA and a high modulus (E=1200 kPa) scaffold made with 0.4 g/mL 5 kDa PEGDA were used.

2.2.3.4 Glass Slide Functionalization

Glass slides functionalized with acrylated-RGD were used as a significantly higher modulus positive control for this work. Glass has a reported elastic modulus in the gigapascal range making the modulus on the order of 10^6 times higher. In addition to the significantly higher modulus, by functionalizing the glass with the same adhesion peptide as the hydrogels, this allows for similar adhesion mechanisms for the cells in all conditions. In order to functionalize glass slides with RGD for cell culture, the surface of the slide had to be acrylated. First, the slide was incubated in a beaker of 25% nitric acid (30% solution) and 75% hydrochloric acid (30% solution) in a sonicator at 50-60°C for 5-10 minutes. After allowing the beaker to cool to room temperature, the slides were removed from the acid solution and washed in ultrapure water for 1 minute in the sonicator bath at 50 kHz. This wash was repeated 3 times. Another wash step was completed using 70% ethanol. The slides were then allowed to dry. Once the slides were completely dry, 50 μL of 0.1% 3-(trimethoxysilyl) propyl acrylate in chloroform solution was slowly pipetted onto the surface of the slide, carefully distributing the solution evenly. The slides dried overnight and were then washed with cold ultrapure water to remove unadsorbed acrylate groups. Finally, to functionalize the surface with Acryl-PEG-RGDS, 10 mM ACRL-PEG-

RGDS in HEPES-buffered saline (10 mM N-[2-hydroxyethyl]piperazine-N0-[2-ethanesulfonic acid] and NaCl in ultra pure water), with 10 μL/mL photoinitiator solution (2,2-dimethoxy-2-phenyl-acetophenone 300 mg/mL in N-vinylpyrrolidone) was slowly pipetted on the glass surface, carefully distributing the solution evenly across the surface. This was then exposed to UV-light for 3 minutes.

2.2.4 Cell Culture

2.2.4.1 ARPE-19 Cell Culture

ARPE-19 cells (ATCC, Manassas, VA, USA) were seeded on scaffolds at 10,000 cells/cm^2. Cells were cultured in DMEM/F12 with 15% v/v fetal bovine serum and 1% v/v antibiotic solution (10,000 Units penicillin and 10 mg streptomycin per mL). Scaffolds were moved to a new well after 8 hours to retain only cells attached to scaffolds and eliminate cells that had attached to well bottoms. Media was changed every other day for 14 days. Cell analyses were conducted on days 1, 7, and 14.

2.2.4.2 Primary Embryonic Chick RPE Cell Isolation & Culture

On embryonic day 6, RPE cells were isolated from chick embryos. RPE isolation was performed following the method outlined by Wang et al. [67]

Briefly, the egg was removed from the incubator and cleared with 70% ethanol. Gently, the top of the shell was cracked with a pair of tweezers and a hole was created by removing pieces of the shell and the vitelline membrane. The embryo was removed and placed in a 60-mm dish with cold 1xPBS. The head of the embryo was then decapitated and the eyes enucleated. The eyes were placed in a separate 60-mm dish sitting on ice. Under the dissecting microscope, the sclera was removed using tweezers and then, an incision was made in the RPE and retina, the lens and peripheral retina was removed. The resulting RPE-retina-vitreous was moved into another dish. The RPE was then separated from the retina and vitreous humor and placed in 10% serum supplemented media. Once isolation was complete, the RPE cells were transferred into a 15 mL tube, washing the 60-mm dish until no cells were visible. The cells were centrifuged at 650 g for 5 minutes and the supernatant was discarded. The cells were then resuspended in complete medium and vigorously pipetted to break up large clumps. These cells were then immediately seeded on scaffolds at 10,000 cells/cm^2. Seeded cells were maintained in DMEM/F12 media with 10% FBS and 1% antibiotic solution.

2.2.5 Cell Analysis

2.2.5.1 Fluorescence Microscopy

Live/Dead® calcein acetoxymethyl (AM) and ethidium homodimer-1 viability/cytotoxicity stain (Life Technologies, Carlsbad, CA, USA) was performed to qualitatively assess cell adherence and viability. Briefly, the ethidium homodimer-1 and calcein AM was added to media in 1:500 (v/v). Scaffolds were incubated in the solution for 10 minutes. Following incubation, cell nuclei were labeled using Hoescht at a 1:5000 (v/v) dilution in PBS. The scaffolds were then washed in PBS and imaged (N=?? total; n=3 for each condition) on an epifluorescent microscope (Axio Observer Z1, Zeiss, Oberkochen, Germany).

In addition to using fluorescent microscopy to assess viability and adhesion, the cytoskeleton of cells on scaffolds was visualized through phalloidin staining of actin using a cytoskeleton staining kit (EDM Millipore, Billerica, MA, USA). Cells were fixed using 4% paraformaldehyde, permeabilized with 0.1% Triton X-100 in PBS, and then blocked using 1% BSA in PBS. The cells were then incubated with a 1:100 TRITC-phalloidin in PBS solution for 60 minutes. Following several washes, cells were incubated with a 1:1000 4',6-diamidino-2-phenylindole (DAPI) in PBS solution for 5 minutes and then imaged on an Olympus IX81 Confocal Microscope.

2.2.5.2 Metabolic Activity Assay

A PrestoBlue mitochondrial reduction assay was performed on days 1, 7, and 14 to determine cellular activity on the scaffolds of varying moduli. Control and experimental scaffolds with cells attached were immersed in assay solution and incubated for 4 hours. Controls were matched molecular weight hydrogels with no cells attached. A 100 μL sample of assay solution was aspirated from each well following the incubation period and pipetted into a fresh 96 well plate then read on a Beckman Coulter DTX 880 Multimode Detector with excitation at 560 nm and emission at 595 nm. The values read for control scaffold fluorescence was subtracted from the values read for experimental scaffold fluorescence (N=15 total; n= 5 for each condition).

2.2.5.3 qPCR

ARPE-19 RNA was isolated using Qiagen RNEasy Plus kit (Qiagen, Hilden, Germany) according to the manufacturer's protocol. Briefly, cells were lysed using β-mercaptoethanol and Qiagen RLT Plus buffer and then centrifuged through a Qiashredder column to remove large debris and contaminants. Genomic DNA was removed using an eliminator column. Following this, ethanol was used to provide binding conditions for RNA to the RNeasy spin column,

while other non-RNA contaminants were then washed away. The RNA was then eluted through the column and quantified using a NanoDrop™ spectrophotometer and associated software. Next, the RNA was normalized to a uniform concentration. Samples were reverse transcribed using the High Capacity cDNA Reverse Transcription Kit (Applied Biostystems). PCR was performed using SYBR Green PCR Master (Applied Biosystems) mix and PikoReal real time PCR system. The fold change relative gene expression compared to that of the control TCPS was determined using the delta-delta Ct method after normalizing to the housekeeping gene, *GAPDH* (N=15 total; n=5 for each condition).

Table 2.1 Primer Sequences for Real-Time PCR

Gene of	**Primer Sequence (5′ to 3′)**
CRALBP	F: AGATCTCAGGAAGATGGTGGAC
	R: GAAGTGGATGGCTTTGAACC
COL-I	F: GTCACCCACCGACCAAGAAACC
	R: AAGTCCAGGCTGTCCAGGGATG
IL-6	F: GGCACTGGCAGAAAACAACC
	R: GCAAGTCTCCTCATTGAATCC
MCP-1	F: GATCTCAGTCAGAGGCTCG
	R: TGCTTGTCCAGGTGGTCCAT
IL-8	F: CTGGCCGTGGCTCTCTTG
	R: TCCTTGGCAAAACTGCACCTT
SMAD3:	F: TCCCCAGCACATAATAACTT
	R: TGGGAGACTGGACAAAAAT
αSMA	F: CTGGCATCGTGCTGGACTCT
	R: GATCTCGGCCAGCCAGATC
GAPDH	F: ACAACAGTCCATGCCATCAC
	R: TCCACCACCCTGTTGCTGTA

2.2.6 Statistical Analysis

Cellular metabolic activity, elastic moduli, and gene expression were compared between the different molecular weight scaffolds using a Student's *t*-test when comparing two groups or an analysis of variance (ANOVA) when comparing more than two groups. Following ANOVA, pairwise comparisons between groups was performed using Tukey's post-hoc analysis. For metabolic activity and gene expression analyses, the dependent variables were control-

adjusted results. *p*-Values less than 0.05 were considered significant and analyses were conducted in Matlab and Microsoft Excel. Statistical significance is indicated in the figures, which are reported as mean ± standard error.

2.3 Results

2.3.1 Mechanical Characterization of Scaffolds

The elastic, or Young's, modulus of scaffolds tested in uniaxial tension was determined following 24 hours of scaffold swelling in PBS. Scaffold modulus was modified through two approaches. The first approach was by varying the PEGDA molecular weight and the second approach was to vary the concentration of PEGDA in solution. Using molecular weights 3.4, 5, 10, and 20 kDa, the Young's modulus can be changed up to two orders of magnitude. The tested scaffolds' elastic moduli varied between 60 kPa and 1200 kPa (Figure 2.4) while the bulk modulus varied between 220 kPa and 3800 kPa (Figure 2.5). As seen in these figures, there was a difference in the Young's modulus measured via tension and compression. This has much to do with the viscoelasticity of the hydrogels, as well as their water content. The largest discrepancy seen is in the 1x concentration of low molecular weight hydrogels. This 1x hydrogel has a higher water content compared to the 2x concentration. In addition, discrepancy likely exists due to different strain rate used in compression and tension. In

viscoelastic materials, force varies with velocity. Therefore, the strain rate variation could cause a discrepancy. Moving forward into cell studies, it was not critical to determine the root cause of the difference between the two methods. However, in further optimization of scaffold modulus, best methods of characterization must be defined.

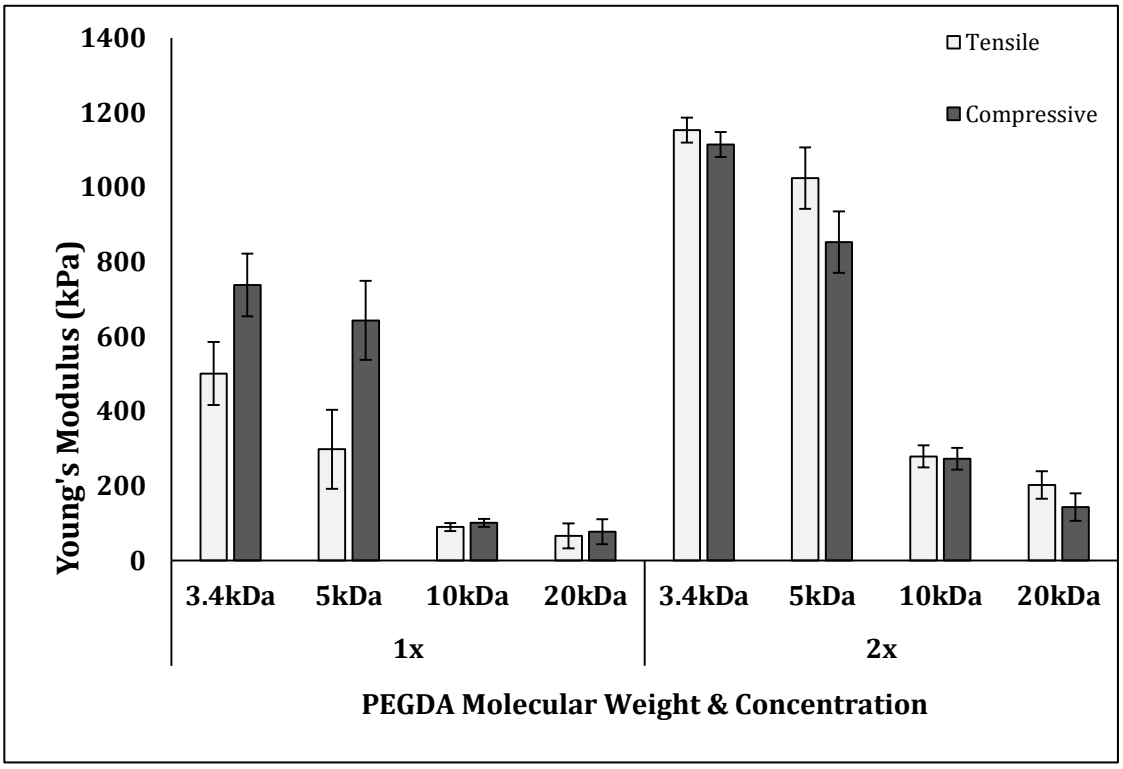

Figure 2.4: Scaffold Young's modulus as determined through tension and compression testing. The modulus varies with PEGDA molecular weight and concentration. Higher PEGDA molecular weight leads to a lower modulus, or a less rigid scaffold. Higher concentrations of PEGDA lead to a higher modulus, or a more rigid scaffold.

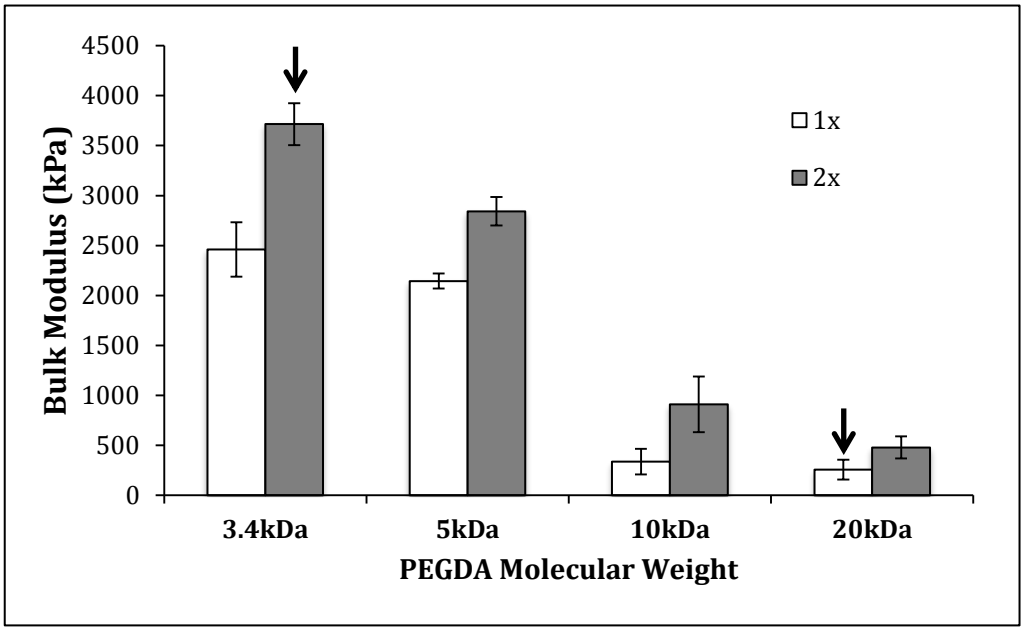

Figure 2.5: Scaffold bulk modulus, like the Young's modulus, varies with both molecular weight and concentration. Bulk modulus was determined using values for E obtained from compression tests and equation 1. Groups indicated with the arrows were used in cell studies.

2.3.2 Fluorescent Microscopy

Following the seeding of cells on low modulus (E=60 kPa, K = 80 kPa) and high modulus (E=1200kPa, K=2000kPa) scaffolds, fluorescent microscopy was performed. These images were analyzed qualitatively to observe differences in cell adhesion patterns. Representative images are shown in Figure 2.6. The cells show a more homogenous spreading on the high modulus scaffold compared to the low modulus scaffold. Cell clusters with a higher percentage of cell death were observed on the low modulus scaffold.

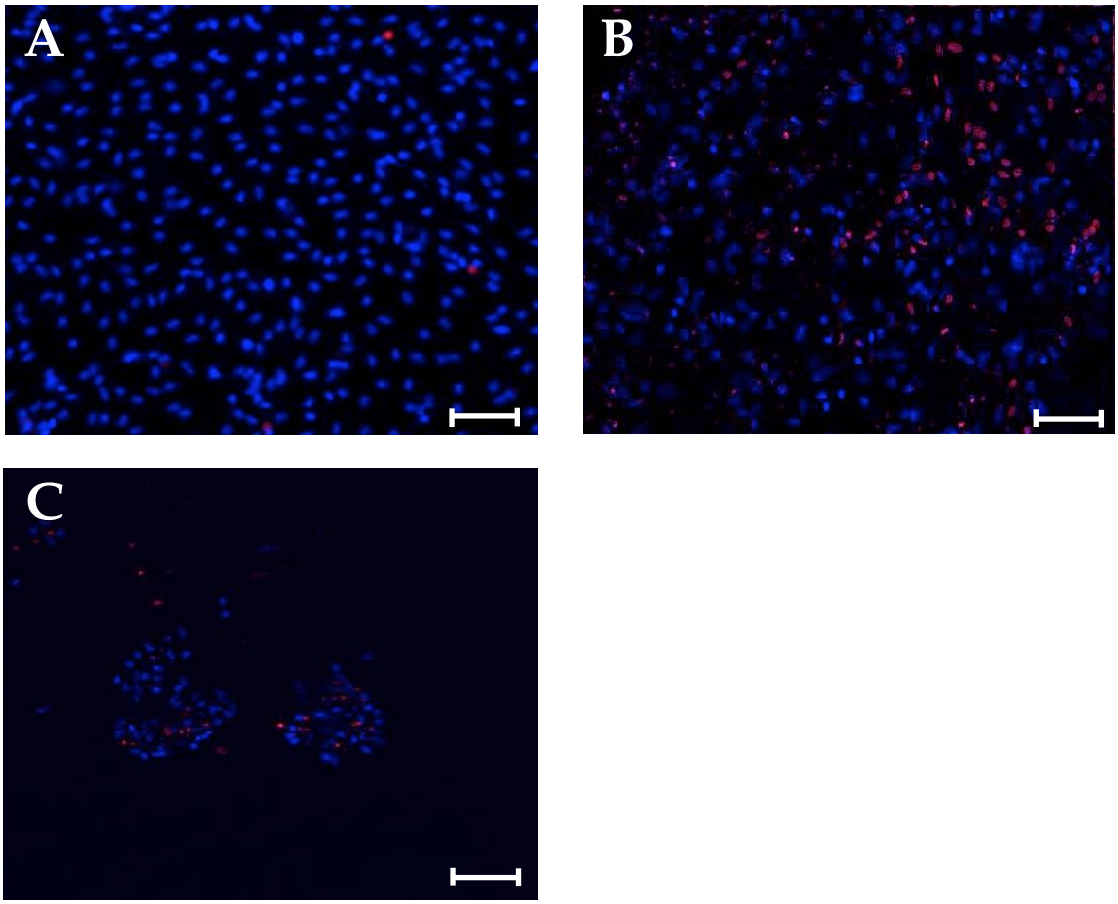

Figure 2.6: ARPE-19 cells on different culture substrates. The ARPE-19 cells formed a confluent monolayer on TCPS with very little cell death (A); the cells still had a high density on the high modulus scaffold, with more noticeable cell death (B); cells formed clumps on the low modulus scaffolds with cell death on the low modulus scaffolds (C). Blue = Hoescht, Nuclear Stain; Red = Ethidium homodimer-1, dead cells. Scale bar 100 μm.

The cytoskeletons of RPE cells on different moduli scaffolds were visualized through fluorescently tagged phalloidin binding to F-actin filaments (Figure 2.7). Comparing cells on the high modulus scaffold to cells on the low modulus scaffold, it is observed that the cells on the low modulus scaffolds exhibit elongated, parallel actin stress fibers by day 7. The cells on the high modulus scaffolds show more peripheral actin fibers, less parallel stress fibers. By day 14, however, the cells on the low modulus detached and only very few cells with poor morphology could be visualized on the scaffold surface. On the high modulus scaffold, cells were still visible, but appeared to lose their peripheral actin filaments as more irregular actin fibers appeared. In comparison, the functionalized glass slide control demonstrated strong peripheral actin fibers even on day 14. The cells on the functionalized glass slide also exhibited the characteristic cobblestone morphology of native RPE cells.

2.3.3 Metabolic Activity

The metabolic activity assay was conducted on days 1, 7, and 14 of culture. Due to number of available cells, these assays were only performed in ARPE-19 cells. Results were normalized to day 1 to determine how the cellular activity changed over the culture period. On both days 7 and 14, the high modulus scaffold resulted in greater cell metabolic activity than all other groups.

On day 7 this increase over control was not statistically significant, but on day 14 it was significantly higher than the other groups. The functionalized glass and TCPS do not show any significant differences at any time points. A change in cell number from day 1 would account for this difference; however, none was seen. There was no noticeable difference in the number of cells on each substrate over the 14 days. After 14 days, the cells on the high modulus scaffold were the only cells with an increase in metabolic activity over day 1 (Figure 2.9).

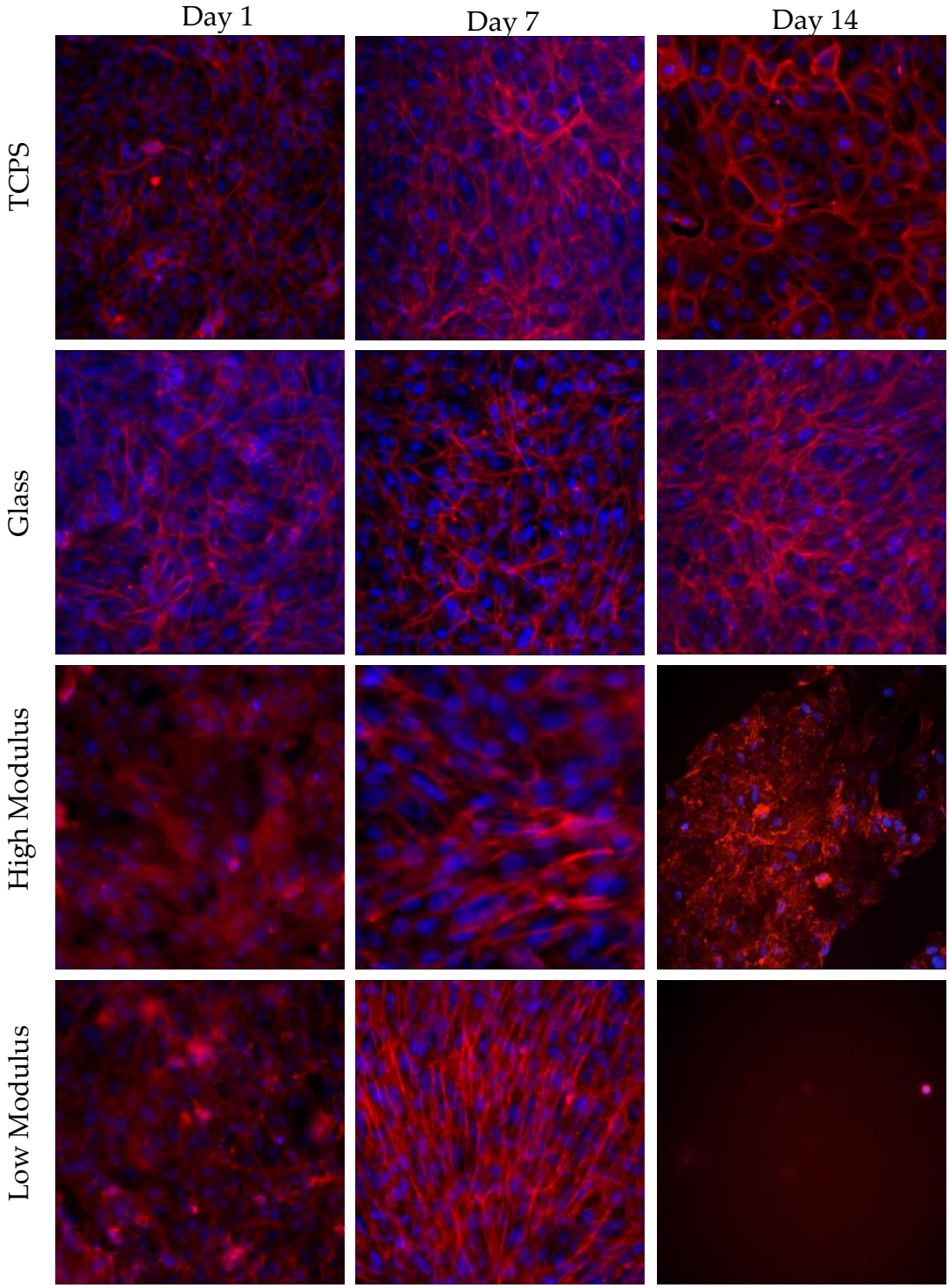

Figure 2.7: Phalloidin staining of the actin cytoskeleton of ARPE-19 cells on various moduli substrate. The ARPE-19 cells demonstrate strong parallel actin stress fibers on low modulus scaffold by day 7 and by day

(Figure 2.7 continued) 14 there is little to no cell attachment. On the high modulus scaffolds, the stress fibers were less pronounced and there was still attachment at day 14.

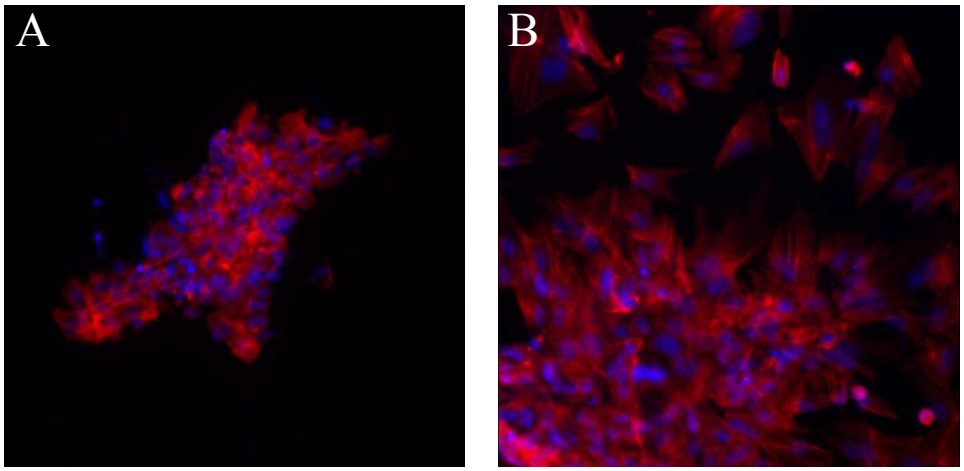

Figure 2.8: Phalloidin staining of the actin cytoskeleton of embryonic chick RPE cells on low modulus (A) and high modulus (B) scaffolds on Day 7. The chick RPE cells demonstrated similar adhesion patterns to the ARPE-19 cells with low modulus scaffolds having more cell aggregation, while high modulus had more cell spreading across the surface.

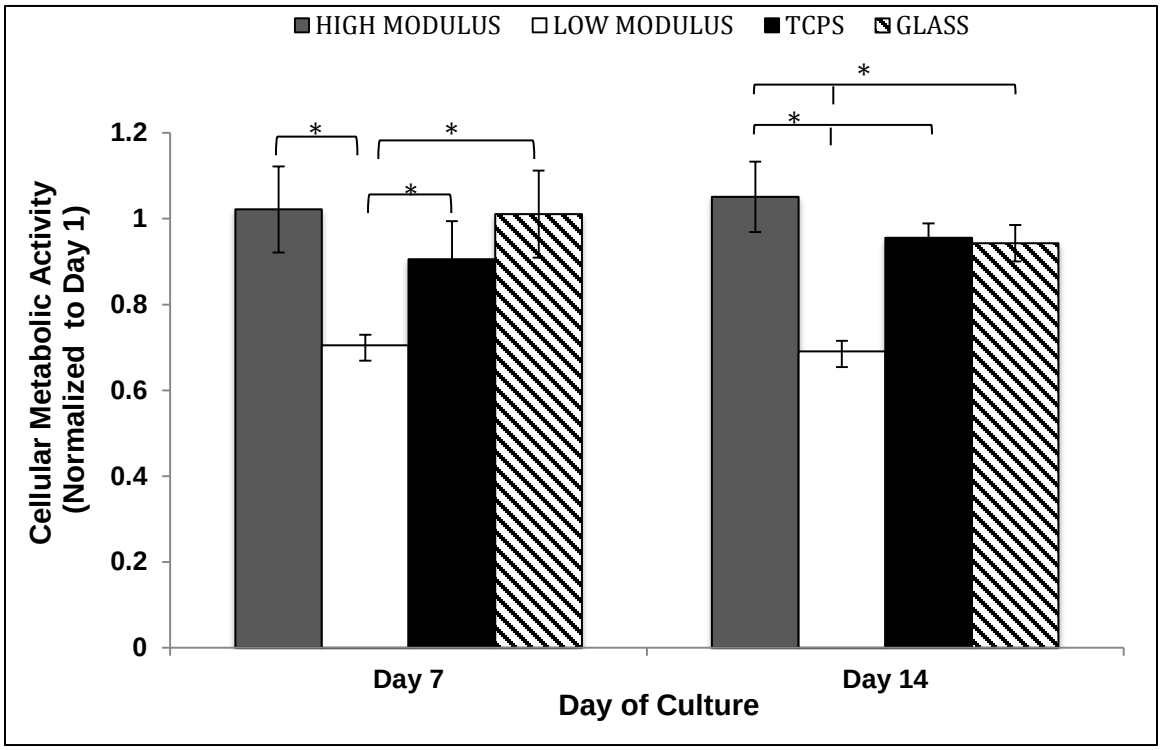

Figure 2.9: ARPE-19 metabolic activity on scaffolds of varying modulus. By day 7 of culture, the cells on the low modulus scaffold had significantly decreased activity when compared to both other conditions. The high modulus and TCPS were not different on day 7. On day 14, all three groups were significantly different from each other with the high modulus scaffold having the highest activity. *$p<0.05$

2.3.4 Gene Expression

The genes investigated in this work can be categorized into two categories: inflammation (IL-6, IL-8, MCP-1) and phenotypic maturity (SMAD3, αSMA, COL-1, CRALBP). Expression levels were measured in ARPE-19 cells since there were not enough embryonic chick RPE cells for analyses. The expression of IL-6 and IL-8, the scaffold groups trended higher than the functionalized glass and TCPS groups. On day 7, the high modulus scaffold had significantly higher expression of IL-8 when compared to all other groups using Student's t-test. No trend emerged in the expression of MCP-1. The expression of αSMA, a dedifferentiation marker, was significantly higher on low and high modulus scaffolds at day 3 but only significantly different on low modulus scaffolds at day 7, while SMAD3, another dedifferentiation marker did not demonstrate significant differences. In addition, collagen type I expression and characteristic RPE gene CRALBP did not demonstrate any significant differences or obvious trends between the groups (Figure 2.10, 2.11, 2.12).

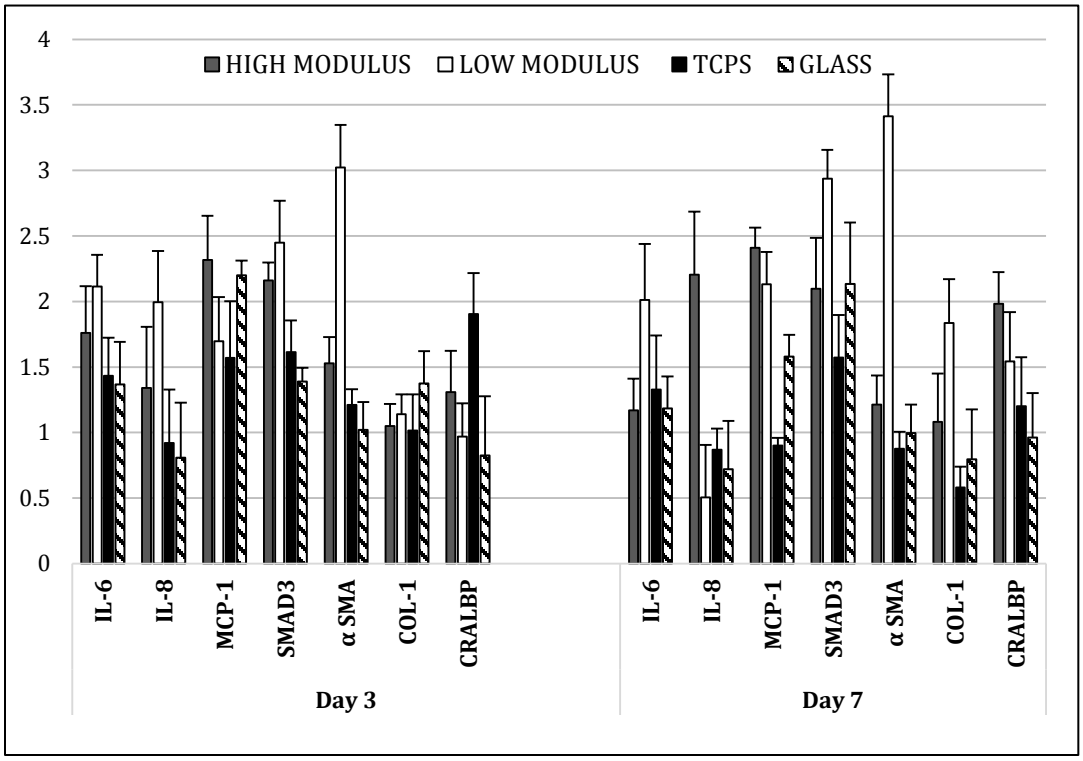

Figure 2.10: Overall results of relative gene expression of ARPE-19 cells on two different modulus scaffolds, functionalized glass slides, and TCPS.

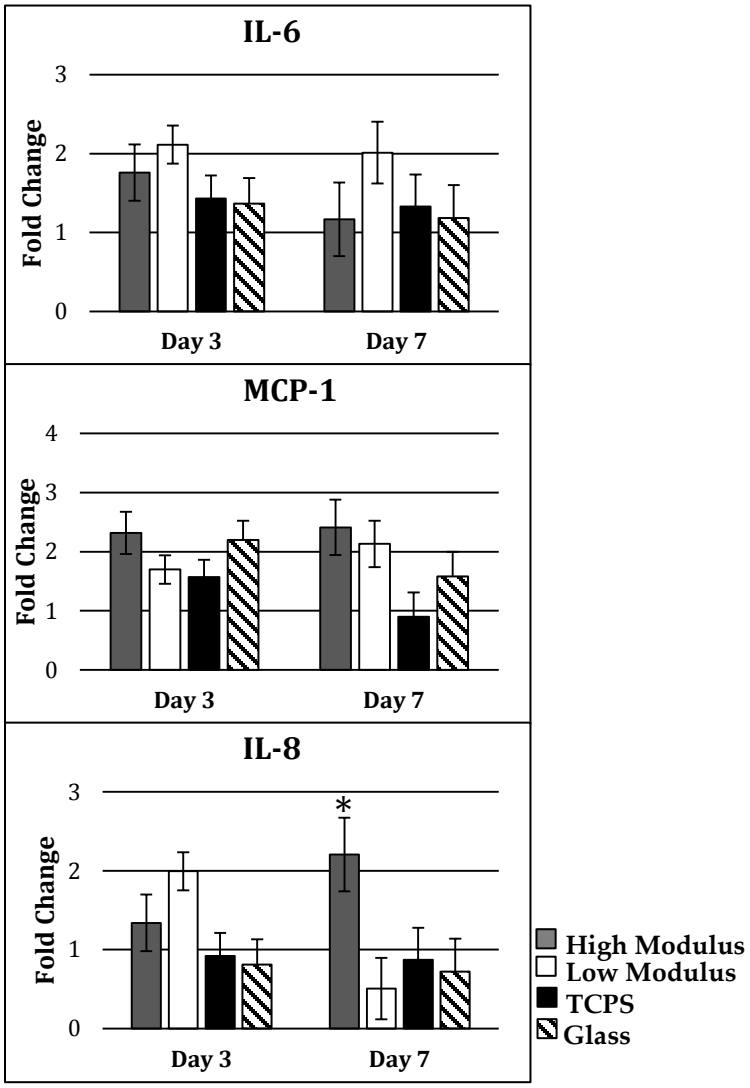

Figure 2.11: qPCR results for ARPE-19 expression of inflammatory markers IL-6, IL-8, and MCP-1 on all substrates. IL-6 and IL-8 trended higher on scaffolds than on the TCPS and glass. On day 7, IL-8 expression on high modulus scaffolds increased from day 3 levels and was significantly higher than on all other substrates ($p<0.01$) while on low modulus scaffolds, day 7 IL-8 expression decreased from day 3 levels. No trend is seen in MCP-1 expression.

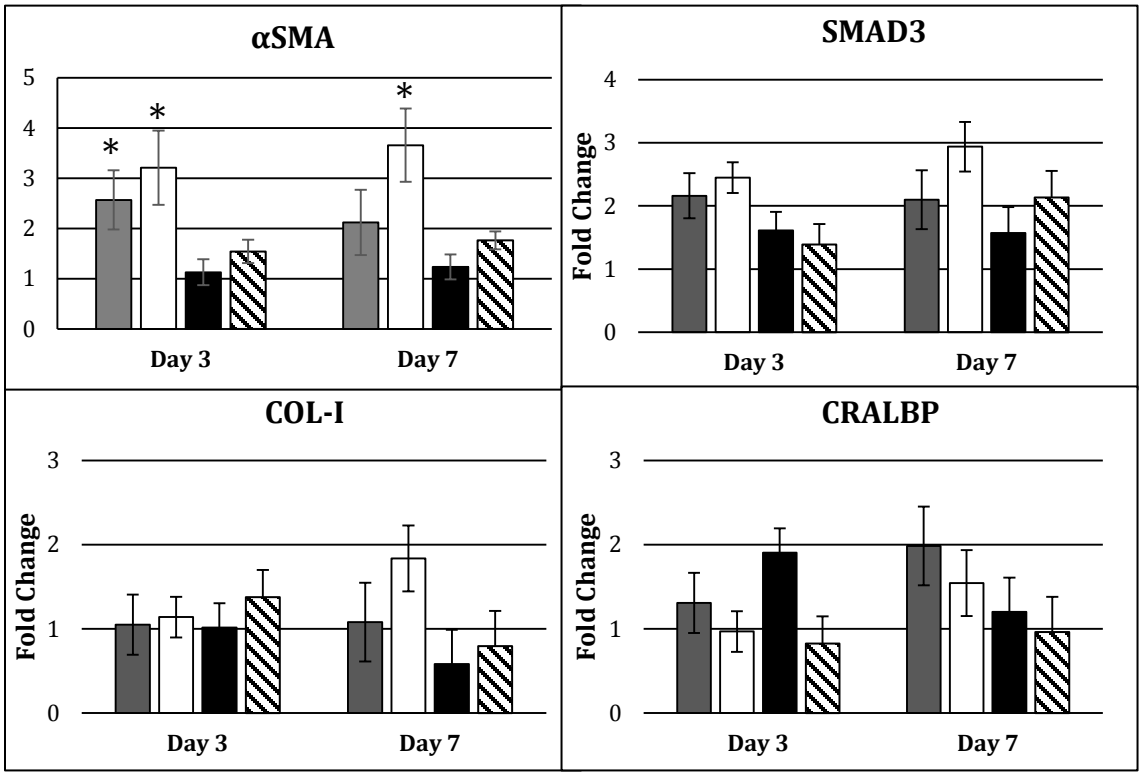

Figure 2.12: qPCR results for ARPE-19 expression of dedifferentiation and maturation genes, *α*SMA, SMAD3, COL-1, and CRALBP. *α*SMA demonstrated significantly higher expression on low modulus and high modulus scaffolds at day 3 but was only different on the low modulus scaffold at day 7, $p<0.01$ for both time points. SMAD3, another dedifferentiation marker, along with COL-I and CRALBP, markers of phenotypic maturity did not show significant differences.

2.4 Discussion

This study demonstrates that the mechanical properties of a scaffold have significant effects on RPE cells. Previously published RPE studies on scaffolds have demonstrated microglial migration and the presence of fibroblast- and macrophage-like cells following implantation. Since IL-6, IL-8, and MCP-1 are microglial and inflammatory cell attractants and αSMA and SMAD3 have been implicated in RPE dedifferentiation into fibroblast- and macrophage-like phenotypes, this study focused on how scaffold modulus affects the expression of these genes in the seeded RPE cells. The increased expression of IL-6 and IL-8 on both scaffolds, suggests that cells seeded on scaffolds could contribute to recruiting microglia and other inflammatory cells *in vivo*. In addition, the significantly higher expression of αSMA on the low modulus scaffold shows that substrate modulus can contribute to dedifferentiation of RPE cells. For the genes in which functionalized glass elicited the lowest fold change, it suggests that the most important criterion is stiffness, and the high modulus scaffolds were not stiff enough. For the genes in which TCP elicited the lowest fold change, it suggests that the cells may have preferred the surface treatment of TCP over RGD as an attachment motif. These results demonstrate the importance of modulus as a design parameter for scaffolds to be used for RPE transplantation.

Through careful design and fabrication of scaffolds, it is possible to control scaffold modulus and, therefore, may be possible to control the expression of these microglial attractants for successful long-term treatment.

The only reported elastic modulus for a BM is that of a porcine BM, which was calculated to be approximately 1000 kPa. [Candiello et al, 2007] One of the goals of this study was to present RPE cells with scaffolds approximating the normal BM Young's modulus, and scaffolds with moduli an order of magnitude above and below the norm. The Low and High modulus scaffolds fabricated in this study achieved Young's moduli an order of magnitude below and at the reported values for the BM Young's modulus. Since it was not possible to achieve a Young's modulus of 10,000 kPa, glass was functionalized identically to the PEG substrates as a substitute. Tensile and compressive data of the scaffolds showed strong correlation for 2x concentration scaffolds at all molecular weights. For 1x concentration scaffolds, the Young's modulus values were the same for 10 and 20 kDa scaffolds, but the values differed for 3.4 and 5 kDa scaffolds. Since viscoelastic effects would be observed more strongly at higher molecular weight hydrogels (which retain more water), it is likely these differences are due to handling difficulties with lower molecular weight 1x scaffolds.

Fluorescent microscopy qualitatively revealed that both ARPE-19, an established RPE cell line, and primary embryonic chick RPE cells had different

adhesion patterns on low modulus and high modulus scaffolds. This similar adhesion behavior in both an immortalized RPE cell line and primary RPE cells confirms that the observed adhesion pattern is not an artifact of ARPE-19 cell line development and propagation. Despite this important finding, the use of embryonic chick RPE cells had several limitations. First, scaffold seeding requires a large number of cells and there is a limited number of cells obtained during isolation and as primary cells, these cells can only be expanded to a certain extent since too many passages alters their behavior. Secondly, there is a limited ability to fully confirm isolation of RPE cells from neural retinal cells and the native Bruch's membrane. These factors would confound results obtained with these cells, and for these reasons embryonic chick RPE cells were not explored further. Rather, RPE cells derived from induced pluripotent stem cells were investigated.

In addition to cell adhesion patterns, fluorescent microscopy demonstrated obvious differences in the orientation of actin fiber filaments of the cytoskeleton. This is a significant observation because early studies on the effects of scaffold modulus on epithelial cells suggest that cells sense their physical environment, causing differences in focal adhesions and expression of intracellular pathways. RPE dedifferentiation has been characterized by a change in expression of cytokeratin proteins, a component of the intracellular cytoskeleton. In addition, it has been established that the actin cytoskeleton

reorganizes from its characteristic hexagonal morphology to a disorganized, random morphology during dedifferentiation. [68] Therefore, it is possible that the mechanical environment experienced by RPE cells affects their adhesion and initiates or promotes dedifferentiation. This is supported by recent work demonstrating difference in phagocytic ability of RPE cells on different substrate moduli. [69]

The cell activity, as measured by a mitochondrial reduction assay, was also affected by the different moduli. Because it remains difficult to quantify cell number on scaffolds, the cell activity was normalized to the Day 1 activity. Therefore, changes in activity can be attributed to either cell number due to proliferation or death, or change in the cell activity itself. By day 7, the cells cultured on low modulus scaffolds had an activity approximately 70% of their day 1 activity. The cells cultured on the high modulus scaffold increased their activity over the 14 day culture period to a level statistically different from the cells on low modulus hydrogels and functionalized glass. This demonstrates that either proliferation is occurring on the high modulus scaffold or the cells are more metabolically active. Since there was no appreciable difference in cell number, the latter is likely.

For the first time, this study reveals the response of RPE cells to changes in scaffold modulus. This study demonstrated that the modulus of a substrate

affects the expression of the microglial attractants, IL-6 and MCP-1. This establishes that scaffold modulus should be considered an important design parameter in scaffolds developed for RPE transplantation. These studies showed it was possible to promote the expression of inflammatory genes in RPE cells simply by altering the mechanical properties of the underlying scaffolds. If scaffold mechanical properties alone can promote the expression of these inflammatory genes *in vitro*, it is reasonable to believe that once implanted into a diseased retina, the inflammatory response will be significant. While SMAD3 did not demonstrate a significant difference between groups, αSMA was significantly higher on low modulus scaffolds at both time points. These results suggest further study into dedifferentiation of RPE cells caused by scaffold modulus is important in order to design an optimized scaffold.

This study demonstrates that modulus is an important design parameter for scaffolds designed for RPE cell transplantation. It is particularly important to consider how the mechanical environment affects the RPE phenotype and expression of inflammatory markers, as these are two challenges RPE scaffolds face in the translation of cell therapies. Further investigation is needed to fully tease out the effects of modulus and move towards scaffold design optimization.

CHAPTER 3 : THE EFFECTS OF ACTIVIN A ON RETINAL PIGMENT EPITHELIAL CELLS GROWN ON SUBSTRATES WITH VARIED MODULI

3.1 Introduction

Activin A is a member of the TGF-β super family of signaling molecules. [70] This super family of molecules participates in several biological processes including cell differentiation and proliferation, inflammatory and immune responses, and apoptosis. [71, 72] Though there are different types of activins, Activin A is the most extensively studied.

The specific effects of Activin A on RPE cells has been demonstrated through several investigations. [53,73] In a study using explant cultures of chick optic vesicles, Fuhrmann et al. demonstrated that in the absence of extraocular mesenchyme signaling, Activin A promotes expression of RPE-specific genes and downregulates expression of neural markers. [73] In a separate study on the effects of Activin A on RPE cells, Sakami et al. investigated the ability of RPE cells to regenerate small defects through transition to a less mature, proliferating phenotype. [53] With the addition of Activin A, the mature RPE lost its competence to transition to the necessary regenerating phenotype. In recent years, Activin A has also proven to be a useful component in the complete media used to differentiate both embryonic and induced pluripotent stem cells into RPE

cells. Idelson et al. demonstrated that the use of Activin A in differentiation media directs stem cells to form mature, functional RPE monolayers. [74] Many groups have adopted this practice in using Activin A to drive stem cells towards the mature RPE phenotype.

With dedifferentiation of cells on scaffolds being a hurdle that must be overcome in this field, the use of a signaling molecule, such as Activin A, to promote the mature, functional phenotype is desirable. Lacking in the literature is an examination of the isolated effects of Activin A; most RPE scaffolds are derived from natural sources or if synthetic, are coated with laminin or another biological protein that may influence RPE behavior. [18,75] Furthermore, no studies explore the combined effects of scaffold stiffness and presence or absence of Activin A. Therefore, this chapter examines the effects on RPE cells when they are cultured on scaffolds and Activin A is added to culture media, covalently bound to scaffolds, or physically entrapped within scaffolds.

3.2 Materials and Methods

All reagents were purchased from Sigma-Aldrich (Saint Louis, MO, USA) and all PEGDA was obtained from Laysan Bio, Inc (Arab, AL, USA) and used as obtained without further purification unless otherwise noted.

3.2.1 Scaffold Fabrication and Glass Functionalization

3.2.1.2 Covalently Bound Activin A Scaffold Fabrication

In order to covalently bind Activin A (R&D Systems, Minneapolis, MN, USA) to the surface of a PEGDA scaffold, the Activin was first conjugated to PEG-acrylate. This occurs through reaction with heterobifunctionalized Acrylate-PEG-Succinimydal Valerate in 1:35 molar ratio at pH 8.0 under argon. The reaction mixer was placed on a rocker on its highest tilt and speed overnight in 4°C cold room. Following the overnight reaction, the pH was titrated back to 7.0 and the solution was frozen at -80°C, lyophilized, and stored at -20°C.

For the purpose of this study, high modulus and low modulus scaffolds were fabricated. These scaffolds were fabricated using a combination of 20 kDa PEGDA (10% w/v) and 3.4 kDa PEGDA (40% w/v). Fabrication was carried out using the same free radical polymerization method outlined in chapter 2. Briefly, PEGDA was dissolved in HEPES-buffered saline with 10 μL/mL photoinitiator solution (2,2-dimethoxy-2-phenyl-acetophenone 300 mg/mL in N-vinylpyrrolidone). This solution was then pipetted into a sterile glass-slide mold constructed of two 25 mm x 75 mm pre-cleaned glass microscope slides separated by a 500 μm thick Teflon spacer. The solution in the mold was exposed to UV light for 3 minutes. Following polymerization, rectangular-shaped

hydrogel scaffolds were removed from the molds with tweezers and fully immersed in 5 mL phosphate buffered saline (PBS) within petri dishes and allowed to swell for 24 hours in a humidified incubator. Following swelling, the ACRYL-PEG-Activin A was conjugated to the scaffold. First the pegylated-Activin A was resuspended at 1 mM in HEPES-buffered saline to create a stock solution. This solution was then diluted to 100 μM and 10 μL/mL of photoinitiator solution was added to it. Slowly, 250 μL of this solution was pipetted across the surface of the scaffold being sure to spread it evenly across the entire surface. The surface was then exposed to UV-light for 3 minutes and placed in PBS in a humidified incubator for 24 hours.

3.2.1.2 Activin A Encapsulation in Scaffolds

To accomplish Activin A (R&D Systems, Minneapolis, MN, USA) encapsulation in scaffolds, Activin A was added to the PEGDA solution for high modulus scaffolds and low modulus scaffolds prior to polymerization such that there was 280 ng Activin A per hydrogel, the equivalent total mass of Activin added to the media condition. Following this addition of Activin A, the polymerization method outlined above was performed.

3.2.1.3 Glass Slide Functionalization

Glass slides functionalized with acrylated-RGD was used as a significantly higher modulus positive control for this work. Glass has a reported modulus in the gigapascal range making the modulus on the order of 10^6 times higher. In addition to the significantly higher modulus, by functionalizing the glass with the same adhesion peptide as the hydrogels, this allows for similar adhesion mechanisms for the cells in all conditions. In order to functionalize glass slides with RGD for cell culture, the surface of the slide was first acrylated. First, the slide was incubated in a beaker of 25% nitric acid (30% solution) and 75% hydrochloric acid (30% solution) in a sonicator at 50-60°C for 5-10 minutes. After allowing the beaker to cool to room temperature, the slides were removed from the acid solution and washed in ultrapure water for 1 minute in the sonicator bath at 50 kHz for 1 minute. This wash was repeated 3 times. Another wash step was completed using 70% ethanol. The slides were then allowed to dry completely. Once drying was complete, 50 μL of 0.1% 3-(trimethoxysilyl) propyl acrylate in chloroform solution was slowly pipetted onto the surface of the slide, carefully distributing the solution evenly. The slides dried overnight and were then washed with cold ultrapure water to remove unadsorbed acrylate groups. Finally, to functionalize the surface with Acryl-PEG-RGDS, 10 mM ACRL-PEG-RGDS in HEPES-buffered saline (10 mM N-[2-hydroxyethyl] piperazine-N0-[2-

ethanesulfonic acid] and NaCl in ultra-pure water), with 10 μL/mL photoinitiator solution (2,2-dimethoxy-2-phenyl-acetophenone 300 mg/mL in N-vinylpyrrolidone) was slowly pipetted on the glass surface, carefully distributing the solution evenly across the surface. This was then exposed to UV-light for 3 minutes and soaked in PBS overnight to remove any unbound RGD.

3.2.2 Confirmation of Activin A Binding to Scaffold

To confirm the binding of acrylated-Activin A to the scaffold surface, an Activin A ELISA (R&D Systems, Minneapolis, MN, USA) was used to determine the amount of Activin A in the supernatant of PBS soaked scaffolds 24 hours after conjugation.

3.2.3 Activin A release profile

Activin A loaded hydrogels were placed in PBS at 37°C and transferred to fresh solutions after 8 hours and daily after that. The amount of protein released into each solution was measured with Activin A ELISA kit (R&D Systems, Minneapolis, MN, USA) for 7 days.

3.2.4 Cell culture

3.2.4.1 Free Activin A in media

ARPE-19 cells (ATCC, Manassas, VA, USA) were seeded on scaffolds at 10,000 cells/cm^2. Cells were cultured in DMEM/F12 with 2% v/v fetal bovine serum, 1% v/v antibiotic solution (10,000 Units penicillin and 10 mg streptomycin per mL), and 100 ng/mL Activin A (HIGHfree, LOWfree). Scaffolds were moved to a new well after 8 hours to retain only cells attached to scaffolds and eliminate cells that had attached to well bottoms. Media was changed every day for 14 days. Cell analyses were conducted on days 1, 3, 7, and 14.

Induced-pluripotent stem cell-derived RPE cells (LAgen Labs, Rochester, MN, USA) were seeded on HIGHcov and LOWcov and control scaffolds at 100,000 cells/cm^2. These cells were cultured in optimized RPE medium, RPEM (LAgen Labs, Rochester, MN, USA) with 1% v/v fetal bovine serum and 100 ng/mL Activin A.

3.2.4.2 Activin A covalently bound or entrapped scaffolds

ARPE-19 cells were seeded on the Activin A loaded or covalently-bound scaffolds at 10,000 cells/cm^2. This was done with both high modulus and low modulus scaffolds (HIGHencaps and LOWencaps, HIGHcov and LOWcov). Cells were cultured in DMEM/F12 with 2% v/v fetal bovine serum and 1% v/v

antibiotic solution. The scaffolds with encapsulated Activin A were placed on transwell membranes. The membranes were lifted and placed in fresh wells, with fresh media daily to encourage Activin A diffusion out of the hydrogel. The media for the scaffolds with covalently bound Activin A was also replaced daily.

3.2.5 Cell analysis

3.2.5.1 Fluorescence Microscopy

The cytoskeleton of cells on scaffolds was visualized through phalloidin staining of actin using a cytoskeleton staining kit (EDM Millipore, Billerica, MA, USA). Cells were fixed using 4% paraformaldehyde, permeabilized with 0.1% Triton X-100 in PBS, and then blocked using 1% BSA in PBS. The cells were then incubated with a 1:100 TRITC-phalloidin in PBS solution for 60 minutes. Following several washes, cells were incubated with a 1:1000 4',6-diamidino-2-phenylindole (DAPI) in PBS solution for 5 minutes and then imaged on an Olympus IX81 Confocal Microscope.

3.2.5.2 Metabolic Activity Assay

A PrestoBlue mitochondrial reduction assay was performed on days 1, 7, and 14 to determine cellular activity on the scaffolds for the three different experimental groups. Control and experimental scaffolds with cells attached

were immersed in assay solution and incubated for 4 hours. Controls were matched molecular weight hydrogels with no cells attached. A 100 μL sample of assay solution was aspirated from each well following the incubation period and pipetted into a fresh 96 well plate then read on a Beckman Coulter DTX 880 Multimode Detector with excitation at 560 nm and emission at 595 nm. The values read for control scaffold fluorescence were subtracted from the values read for experimental scaffold fluorescence (N=21 total; n= 3 for each condition).

3.2.5.3 qPCR

ARPE-19 RNA was isolated using Qiagen RNEasy Plus kit (Qiagen, Hilden, Germany) according to the manufacturer's protocol. Briefly, cells were lysed using β-mercaptoethanol and Qiagen RLT Plus buffer and then centrifuged through a Qiashredder column to remove large debris and contaminants. Genomic DNA was removed using an eliminator column. Following this, ethanol was used to provide binding conditions for RNA to the RNeasy spin column, while other non-RNA contaminants were then washed away. The RNA was then eluted through the column and quantified using a NanoDrop™ spectrophotometer and associated software. Next, the RNA was normalized to a uniform concentration. Samples were reverse transcribed using the High Capacity cDNA Reverse Transcription Kit (Applied Biostystems). PCR was

performed using SYBR Green PCR Master (Applied Biosystems) mix and PikoReal real time PCR system. The fold change relative gene expression compared to that of the control TCPS was determined using the delta-delta Ct method determining fold change compared to the housekeeping gene, *GAPDH* (N=15 total; n=3 for each condition). The expression was then normalized to day 1 expression to determine how the expression changed through the days of culture. Primer sequences are outlined in Table 3.1.

Table 3.1: PCR primer sequences

Gene of	**Primer Sequence (5′ to 3′)**
CRALBP	F: AGATCTCAGGAAGATGGTGGAC
	R: GAAGTGGATGGCTTTGAACC
COL-I	F: GTCACCCACCGACCAAGAAACC
	R: AAGTCCAGGCTGTCCAGGGATG
IL-6	F: GGCACTGGCAGAAAACAACC
	R: GCAAGTCTCCTCATTGAATCC
MCP-1	F: GATCTCAGTCAGAGGCTCG
	R: TGCTTGTCCAGGTGGTCCAT
IL-8	F: CTGGCCGTGGCTCTCTTG
	R: TCCTTGGCAAAACTGCACCTT
SMAD3:	F: TCCCCAGCACATAATAACTT
	R: TGGGAGACTGGACAAAAAT
αSMA	F: CTGGCATCGTGCTGGACTCT
	R: GATCTCGGCCAGCCAGATC
GAPDH	F: ACAACAGTCCATGCCATCAC
	R: TCCACCACCCTGTTGCTGTA

3.2.5 Statistical Analysis

ELISA results, cellular metabolic activity, and gene expression were compared between groups using a Student's *t*-test when comparing two groups or an analysis of variance (ANOVA) when comparing more than two groups. Following ANOVA, pairwise comparisons between groups was performed using Tukey's post-hoc analysis. For metabolic activity and gene expression analyses, the dependent variables were control-adjusted results. *p*-Values less than 0.05 were considered significant and analyses were conducted in Matlab and Microsoft Excel. Statistical significance is indicated in the figures or figure legends, which are reported as mean ± standard error.

3.3 Results

3.3.1 Confirmation of Activin A Binding

Following covalent binding of acrylated-Activin A to the scaffold surface and 24 hours of soaking in PBS, the supernatant solution was removed from the scaffolds and Activin A concentration of the supernatant was determined using ELISA. This allowed for determination of the amount of Activin A bound to the surface of the scaffold. The results demonstrate that the concentration of Activin A in the starting acrylated-Activin reaction product was 990 ng/mL. This means that 24% of Activin was lost during the reaction and freeze-drying process. The

scaffold supernatant had 28 ng/mL and 41 ng/mL for high and low modulus scaffolds, respectively. From this it was determined that approximately 220 ng of Activin A was conjugated to the high modulus scaffold surface and 206 ng of Activin A conjugated to the low modulus scaffold.

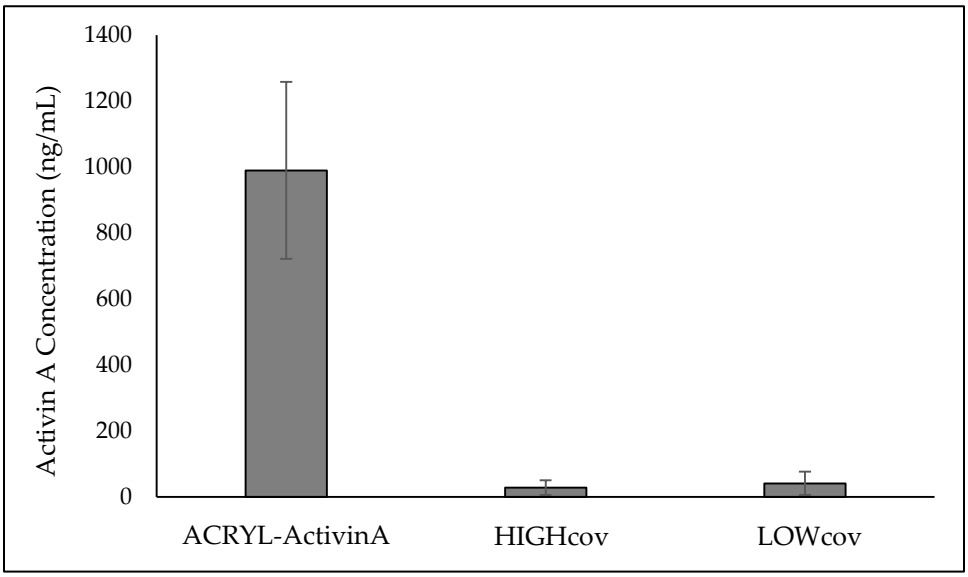

Figure 3.1: Concentration of Activin A in the starting solution (Acryl-Activin A) and in the supernatant following binding reaction to the surface of the hydrogels (HIGHcov and LOWcov). There was very little Activin A in the supernatant and based on this concentration, it was determined that 220 ng and 206 ng of Activin was conjugated to the high and low modulus scaffold surface, respectively.

3.3.2 Encapsulated Activin A Release

Over the 7 days, there was consistent Activin A release from the scaffolds. By day 8, the Activin A concentration was not detectable. Calculating the cumulative mass over the 7 days showed that 88% and 91% of the Activin encapsulated was released from the scaffolds from the high and low modulus scaffold, respectively. As expected, during the first 8 hours, the release of Activin A was significantly higher than all other time points. There was no significant difference between the high modulus and low modulus hydrogels in their release profiles. There was a decaying release profile out of both hydrogels.

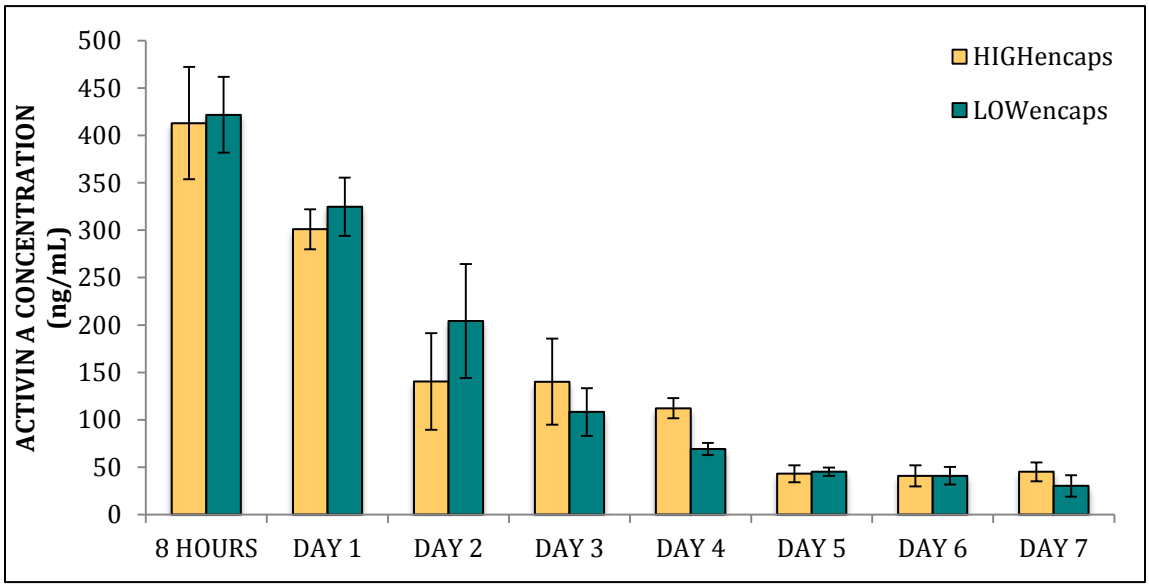

Figure 3.2: Activin A release profile from high and low modulus scaffolds with encapsulated Activin A. There was no significant difference between the two scaffold groups. HIGHencaps refers to high modulus scaffolds; LOWencaps refers to low modulus scaffolds.

3.3.3 Cell Analysis

3.3.3.1 Metabolic Activity

The metabolic activity assay was conducted on days 1, 7, 14 of culture. Results were normalized to day 1. The ARPE-19 cells cultured on high modulus scaffolds exposed to both free and encapsulated Activin A demonstrated significantly higher metabolic activity compared to cells on low modulus scaffolds exposed to Activin A. There were no significant differences between the two high modulus scaffold groups or the high modulus scaffold groups and the functionalized glass. The cells on the low modulus scaffolds had a decreased activity on day 7 and demonstrated further decrease on day 14. (Figure 3.3)

While the cells in the free and encapsulated Activin A groups demonstrated metabolic activity, cells in the covalently bound Activin A group showed no metabolic activity in either the ARPE-19 cells or the iPSC cells. This lack of metabolic activity was also observed for all iPSC-derived RPE cells seeded on scaffolds. The iPSC-derived RPE cells demonstrated no appreciable adhesion to any of these scaffolds.

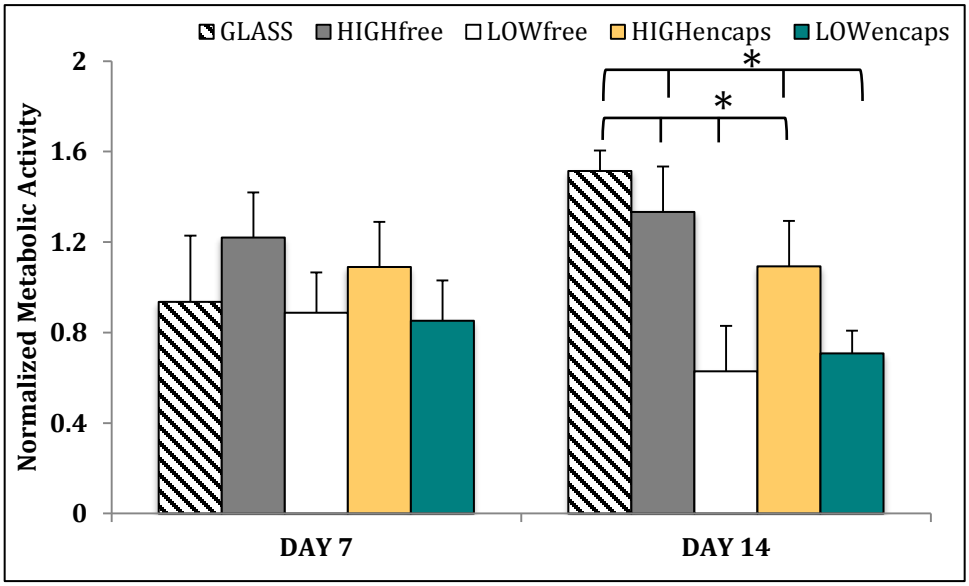

Figure 3.3: Metabolic activity of ARPE-19 cells on varying substrates exposed to Activin A. By day 14, the low modulus scaffolds with free or encapsulated Activin A had significantly lower metabolic compared to all other groups ($p<0.05$).

3.3.3.2 Fluorescent microscopy

HIGHfree and LOWfree, HIGHencaps and LOWencaps, and functionalized glass slides were seeded with both ARPE-19 and iPSC-derived RPE cells. The cells were then grown in their respective media formulations and fluorescent microscopy was performed to determine qualitative differences in

cytoskeleton structure. While ARPE-19 cells demonstrated robust adhesion to the scaffolds surfaces at day 1, the iPSC-derived RPE cells demonstrated no cellular activity or nuclei staining on the surface, indicating lack of cell attachment. The ARPE-19 cytoskeleton on both high modulus scaffold groups and functionalized glass slides demonstrate a more characteristic epithelial morphology through the 14 day culture. This is indicated by more peripheral cytoskeleton. The low modulus scaffolds demonstrated parallel actin stress fibers across the cell body. In addition, by day 14, there were little to no cells present on the low modulus scaffolds of either group (Figure 3.4). The lack of cell adhesion on covalently bound Activin A scaffolds, first indicated via metabolic assay, was further confirmed with fluorescent microscopy. Scaffolds with Activin A bound to the surface did not stain for cell nuclei or cytoskeleton presence.

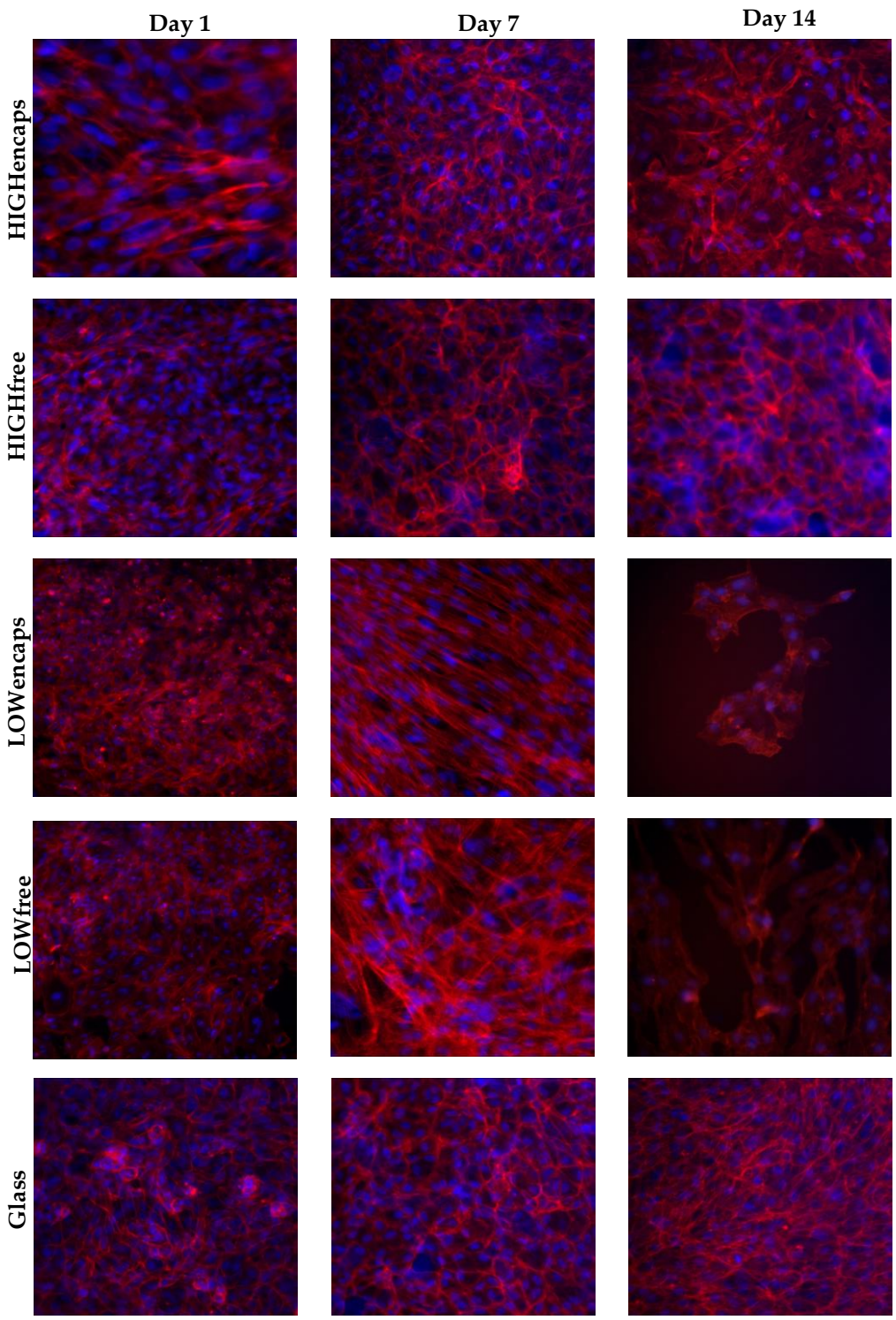

Figure 3.4: Actin cytoskeleton staining of ARPE-19 cells on scaffolds with free or encapsulated Activin A or functionalized glass with free

(Figure 3.4 continued) Activin A. Cells on low modulus scaffolds had strong parallel actin fibers while high modulus scaffolds and glass demonstrated peripheral actin fibers characteristic of the epithelial cells. LOWfree, LOWencaps, HIGHfree, HIGHencaps refer to low modulus scaffolds with Activin A in the media or encapsulated and high modulus scaffolds with Activin A in the media or encapsulated, respectively.

3.3.3.3 Gene Expression

Expression of genes associated with inflammation and cell maturity was determined in ARPE-19 cells using qPCR. The expression of inflammatory genes, IL-6, IL-8, and MCP-1 were higher on low modulus scaffolds at all time points. The expression of dedifferentiation markers, SMAD3 and αSMA, was also significantly higher on low modulus scaffolds. While αSMA demonstrated significantly higher expression at both time points, SMAD3 was only significant at Day 7. High modulus scaffolds showed no obvious trend in genes associated with inflammation. However, both the HIGHfree and HIGHencaps groups demonstrated similar expression patterns of SMAD3 and αSMA compared to the

glass slides. The expression of these dedifferentiation markers was significantly lower compared to the low modulus scaffolds.

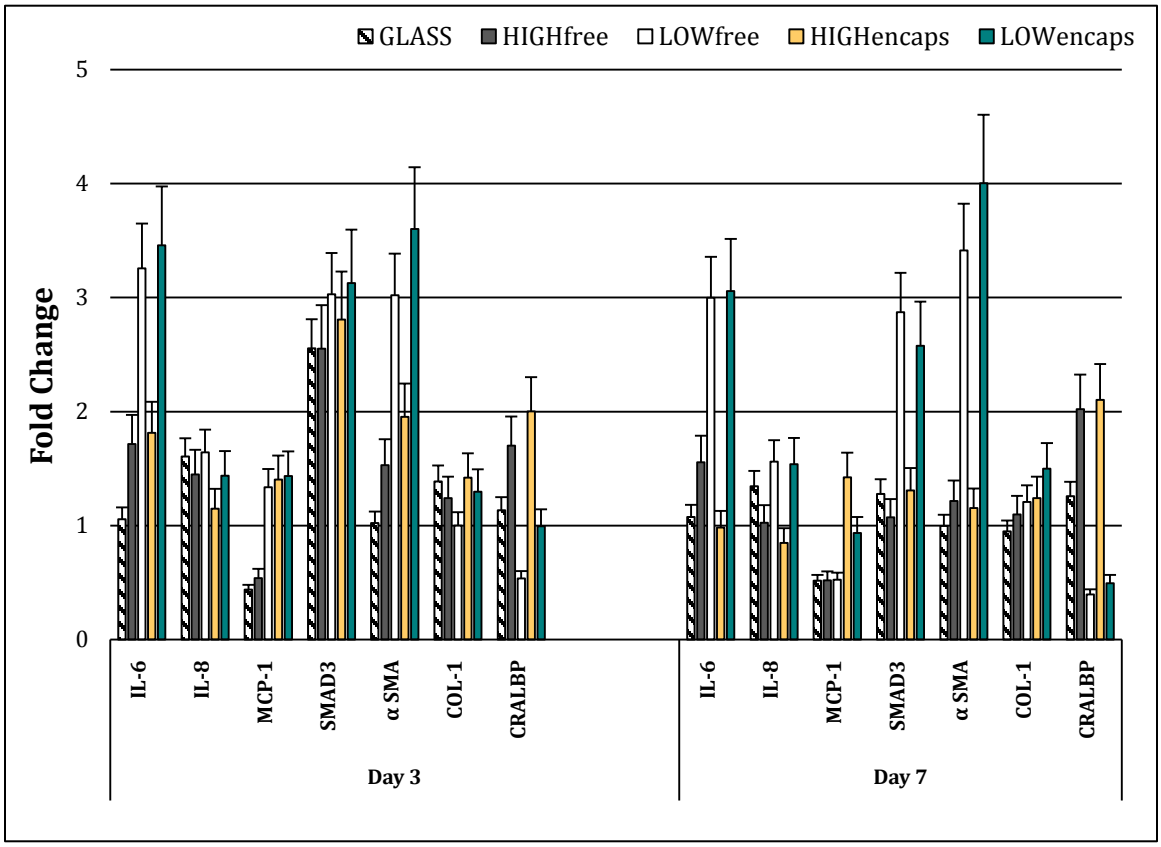

Figure 3.5: Gene expression of ARPE-19 cells on varying substrates exposed to Activin A. Low modulus scaffolds with free Activin A and encapsulated Activin A demonstrated significantly higher expression of IL-6, an inflammatory marker, and αSMA, a dedifferentiation marker compared to both high modulus groups and the functionalized glass. Cells on high modulus scaffolds had significantly higher expression of CRALBP, a characteristic RPE marker, when compared to the low modulus scaffold groups.

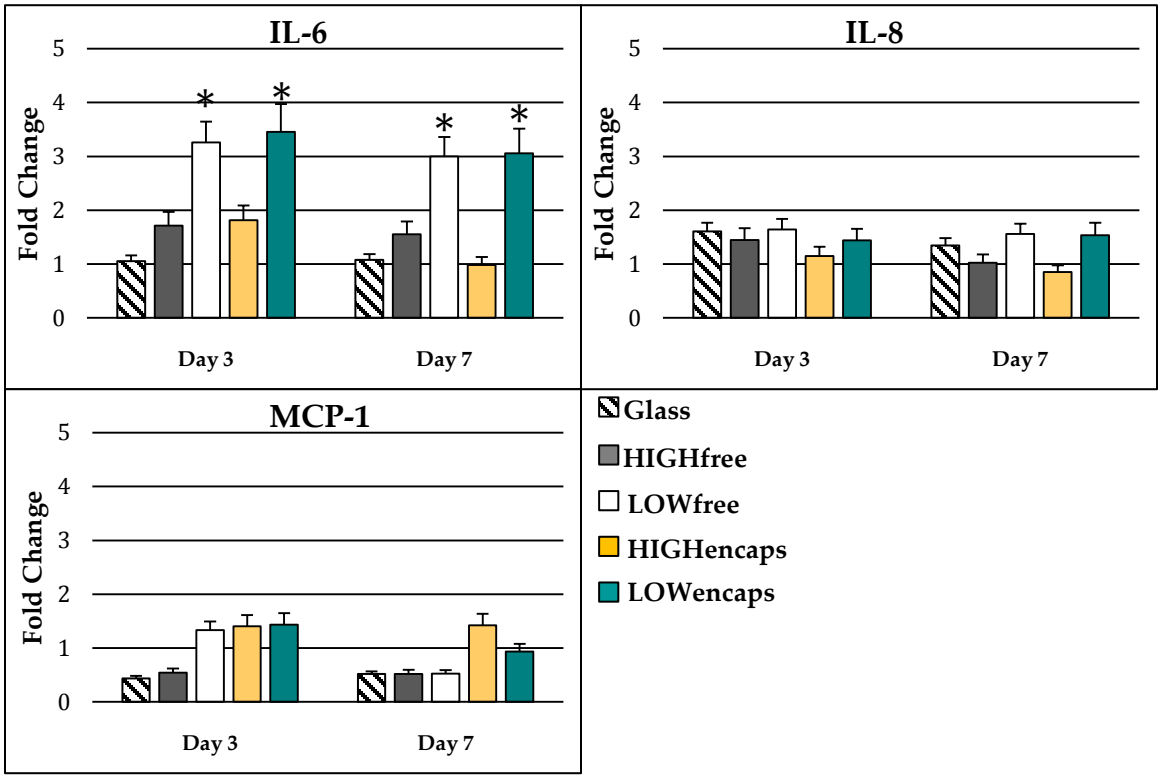

Figure 3.6: Expression of inflammatory genes in ARPE-19 cells on varying substrates exposed to Activin A. Low modulus scaffolds with free Activin A and encapsulated Activin A demonstrated significantly higher expression of IL-6 at both time points.

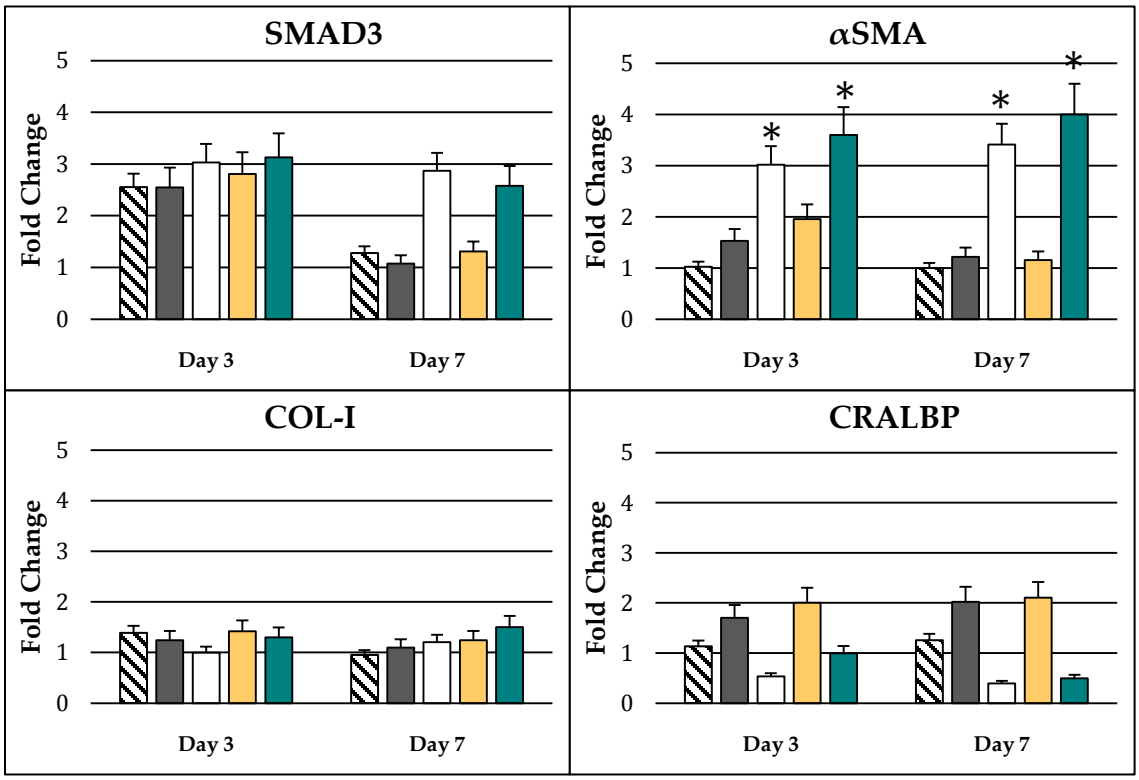

Figure 3.7: Expression of dedifferentiation and phenotypic maturity genes of ARPE-19 cells on varying substrates exposed to Activin A. Low modulus scaffolds with free Activin A and encapsulated Activin A demonstrated significantly higher expression of the dedifferentiation marker αSMA at both time points.

3.4 Discussion

Prior studies in this dissertation demonstrated that substrate modulus affected the adhesion, morphology, and expression of dedifferentiation markers in RPE cells. Activin A is a signaling molecule known to promote the mature RPE phenotype and the present study examined whether chemical stimulation with Activin A could rescue the poor adhesion, morphology, and apparent dedifferentiation of ARPE-19 cells observed on varying substrate moduli. Activin A supplemented media, Activin A encapsulated in scaffolds, and Activin A covalently bound to scaffolds were studied. This work revealed that gene expression of ARPE-19 cells on low modulus scaffolds demonstrated significantly higher inflammatory markers, IL-6 and IL-8, and dedifferentiation markers, SMAD3 and αSMA, compared to high modulus scaffolds and functionalized glass slides. This was true for both the scaffolds exposed to free Activin A, as well as the scaffolds with encapsulated Activin A. The presence of Activin A did not significantly change the expression of cells compared to cells with no chemical stimulation grown on low modulus scaffolds (Chapter 2). The high modulus scaffolds, both with free Activin A and encapsulated Activin A, did not show any significant differences when compared to the functionalized glass slides. When first comparing high modulus scaffolds with free or encapsulated Activin A to high modulus scaffolds with no chemical stimulation

(Chapter 2), a trend emerged showing a lower expression of dedifferentiation markers. In addition to this trend, the expression of CRALBP, the characteristic RPE gene, was consistently higher when the cells were exposed to Activin A.

Previous work demonstrated that actin cytoskeleton reorganization occurred during dedifferentiation, whereby the dedifferentiated RPE phenotype had elongated, linearly arranged actin fibers that spanned across the cytoplasm of the cell. [65] These linear fibers are seen clearly in ARPE-19 cells grown on low modulus scaffolds with both free and encapsulated Activin A. By day 14, most of the ARPE-19 cells had detached from low modulus scaffolds. In the high modulus groups, this cell line demonstrated a more circumferential cytoskeleton. However, when grown on HIGHencaps, ARPE-19 cells demonstrated less epithelial morphology on Day 14 compared to HIGHfree. This is likely due to the reduced release of Activin A from scaffolds after Day 4 of culture.

Both ARPE-19 cells and iPSC-derived RPE cells demonstrated no adherence, even at day 1, to scaffolds with covalently bound Activin A. This indicates that covalent functionalization may not be a good approach for this system. While more characterization must be done to determine the mechanism preventing cell attachment, steric hindrance of the RGD adhesion sites is a concern due to the size of Activin A relative to RGD. In addition to not adhering to covalently bound scaffolds, the iPSC-derived RPE cells did not adhere to the

other scaffolds groups in this study or to the glass slides. These cells are more sensitive to culture environment and this work indicates that a synthetic polymer scaffold with cell adhesion mediated by RGD alone is not sufficient to promote iPSC-derived RPE adherence and growth. Previous studies with these cells used larger cell adhesion molecules including laminin and fibronectin. [18, 75] Functionalizing PEG hydrogels with complete adhesion proteins may be necessary in order to move forward with this cell type on PEG hydrogels. However, the importance of proper controls to understand if these natural cell adhesion molecules are providing more than just attachment sites but biochemical cues to the RPE cells cannot be overstated.

The results of this study demonstrated several important findings. First, low modulus scaffolds increase inflammation and dedifferentiation marker expression and this cannot be rescued using Activin A. This means that modulus stiffness alone can have a dominating effect over exogenous stimulation and should be carefully considered during scaffold design. The second finding is that when cultured on scaffolds with an appropriate modulus, exogenous factors, such as Activin A, can affect cell expression, morphology, and activity. In other words, scaffold modulus alone is necessary to preserve RPE fate, but not sufficient—while the wrong scaffold modulus can have devastating effects on RPE survival regardless of the presence of Activin A, the right scaffold modulus

is necessary, but not enough to ensure RPE survival and requires additional factors such as Activin A. These findings support future work in the field to determine key growth factors and signaling molecules to encapsulate in scaffolds, covalently bind to scaffolds, or deliver into the subretinal space with a cell-scaffold complex to decrease inflammation and promote mature, functional RPE cells post-transplantation.

CHAPTER 4 : CONCLUSIONS AND FUTURE DIRECTIONS

4.1 Dissertation Summary

The broad goal of this dissertation is to understand how cells are affected by the mechanical properties of synthetic polymer scaffolds upon which they are grown and how Activin A affects cells on these various moduli scaffolds. Previous work has established that the transplantation of RPE cells with a scaffold may be more beneficial in treating retinal degenerative diseases than free cells alone. [76] However, there are still several hurdles that must be overcome in order to make cell-scaffold transplantation a long-term therapy for retinal degenerative diseases. First, following the transplantation of cell-scaffold complexes into animal models, inflammation including the migration of macrophages and microglial cells are observed. [18-20, 37, 38] In addition, other inflammatory responses, such as glial scarring, have been reported. [77-79] Secondly, transplanted RPE cells have been observed to migrate and dedifferentiate *in vivo*. [42] The dedifferentiated phenotypes of the transplanted cells have been observed in the host neural retina. [41] This both limits rescue effects of the transplant and causes additional damage to the host neural retina. [79] This work, for the first time, studied the effects of scaffold modulus on inflammation and dedifferentiation of RPE cells grown on synthetic polymer

scaffolds. This study also investigated how Activin A, a molecule known to promote the mature RPE phenotype, affects cells on various moduli scaffolds.

In tissue engineering, scaffold modulus has long been considered an important design parameter for many cell types, particularly epithelial cells . [59-60,80] However, in the retinal tissue engineering field, this parameter has not been investigated fully. In one of the few studies on this topic, Boochoon et al. demonstrated that the elastic modulus of a scaffold influences the cells' ability to phagocytose waste. [69]. Though the Boochoon study suggested scaffold moduli affected the phenotype, no definitive study varied scaffold moduli and examined the effects on RPE gene expression as this study has. Therefore, a driving factor in this dissertation was to fill this gap in knowledge. A main hypothesis of this study is that scaffold modulus affects RPE expression of genes associated with dedifferentiation pathways. The work in this dissertation established that low modulus scaffolds had significantly higher expression of αSMA, a known dedifferentiation marker. [64-65] In addition to this increased expression, the cytoskeleton of cells on low modulus scaffolds demonstrated strong parallel actin stress fibers across the cytoplasm compared to circumferential, peripheral actin fibers indicative of a more mature epithelial phenotype seen on the high modulus scaffolds and the functionalized glass control. [65] The strong parallel fibers have previously been seen in dedifferentiated RPE cells by Grisanti et al.

The results of this dissertation confirm the hypothesis that a scaffold's modulus does affect RPE phenotype and can promote dedifferentiation.

Activin A, known for promoting the mature RPE phenotype was selected to determine if this signaling molecule could rescue the dedifferentiation observed on low modulus scaffolds. Activin A, a member of the TGFβ super family, is often used in differentiation protocols to push stem cells towards mature RPE cells; it has also been shown to promote the RPE phenotype in culture. [53, 73] Of the various moduli substrates examined, the impact of Activin A was observed on high modulus scaffolds. In comparing Activin A exposed cultures on high modulus scaffolds (Chapter 3) to cultures receiving no Activin A (Chapter 2), cultures with Activin A showed a decreased expression of SMAD3, a dedifferentiation pathway. It also demonstrated decreased expression of inflammatory marker, IL-8. In addition, the cytoskeleton of cells on scaffolds exposed to Activin A demonstrated a more epithelial morphology. However, these reductions in dedifferentiation were not seen when cells were cultured low modulus scaffolds. The cells on low modulus scaffolds demonstrated no rescue through Activin A chemical. In this case, the effects of the mechanical environment were dominant over the effects of chemical stimulation.

4.2 Contribution to the Field

The work of this dissertation for the first time studied the effects of mechanical environment on specific dedifferentiation and inflammation markers of ARPE-19 cells, primary chick RPE cells, and iPSC-derived RPE cells. This system proved to not be optimal for work with iPSC-derived RPE cells as scaffolds with RGD alone at 10 mM concentration were insufficient to promote adhesion. However, this scaffold system did reveal significant data with the ARPE-19 cell line. By using PEGDA with controlled cell adhesion peptide conjugation, this work, for the first time in this field, isolated the mechanical properties of the scaffold to study RPE cells grown in these varied environments. By using this synthetic scaffold and short peptide sequence combination, not a high molecular weight extracellular matrix protein, this eliminated the variability of biochemical cues through those long chain proteins. In addition, using synthetic PEGDA scaffolds limited batch to batch variability, often seen in natural polymer systems. This is the first time in this field such a system has been used to study how the mechanical properties affected RPE cell adhesion and gene expression, specifically of inflammatory and dedifferentiation genes.

While Activin A is often used in the field to promote stem cell differentiation towards the mature RPE phenotype, it has not previously been used in a scaffold system. Through the studies conducted with Activin A, several

key contributions were made. First, surface functionalization with covalently bound Activin A may inhibit cell adhesion. While this approach should be explored further, adhesion to scaffolds with surface bound Activin A was minimal for both ARPE-19 cells and iPSC-derived RPE cells . Steric hindrance of adhesion is a possibility as Activin A is a large protein complex. Secondly, through this work, it was demonstrated that the mechanical stimulation cells receive from culture substrate can be a dominant cue relative to chemical stimulation from Activin A. This was demonstrated through the lack of rescue of RPE cells on low modulus scaffolds. When stimulated with Activin A, these cells continued to demonstrate significantly higher expression of dedifferentiation markers. These results are significant as researchers seek to optimize scaffold design and culture conditions for RPE cell expansion and transplantation.

4.3 Future Directions

The work presented in this dissertation serves as a foundation for further optimization of scaffold properties for long-term RPE transplantation success. Potential future work to build on this dissertation includes (1) optimization of chemical and mechanical stimulation of RPE cells and (2) further understanding of key dedifferentiation pathways.

4.3.1 Mechanical and chemical optimization

This work analyzed a low modulus scaffold at 60 kPa, a high modulus scaffold at 1200 kPa, and the significantly higher modulus experimental group of functionalized glass. Further work should be conducted with more moduli scaffolds. By using more moduli, eventually research will reveal an optimal scaffold modulus for culturing and transplanting RPE cells. Although it was not possible to fabricate a 10,000+ kPa scaffold with linear PEGDA, this may be possible with 4- or 8-arm PEGDA, which increases the crosslinking density of the hydrogel. The greater the crosslinking density, the stiffer the hydrogel. In this dissertation, increasing the crosslinking density was achieved by increasing the concentration of the PEGDA and/or by decreasing the molecular weight. Repeating the scaffold design studies using multi-arm PEGDA molecules may permit the fabrication of a PEG hydrogel substrate with a stiffness between the 1200 kPa scaffold developed in this study and glass.

In addition to mechanical environment optimization, chemical environment optimization is another strategy that can be employed to design a long-term therapy. While Activin A alone affects cells on high modulus scaffolds, many other molecules could be used to stimulate RPE cells. Though many growth factors and signaling molecules have not been used in a scaffold system before, it would be pertinent to start with the signaling molecules used to push

stem cells towards the mature phenotype in culture. This would include more studies with Activin A and nicotinamide, as these two signaling molecules have become common in the field. [81] Other options for chemical stimulation would be to introduce epidermal growth factor early in culture to promote proliferation then remove that cue to add a molecule to promote maturation. [54] If the covalent surface modification approach is pursued, because of the potential steric hindrance of cell adhesion, a larger adhesion protein or peptide should be considered for use with Activin A, preferable a molecule similar in size to Activin A. This could circumvent any potential steric hindrance between a large Activin A molecule and smaller adhesion molecules and thus overcome the lack apparent of available adhesion sites on the surface and promote better cell adhesion. It is likely that several signaling molecules, the timing of their stimulation, and proper promotion of cell adhesion during culture must be optimized for the desired RPE behavior. Through this "cocktail" of cues, both chemical and mechanical, researchers will be able to control RPE cell expression, reach a mature functional state faster *in vitro,* and promote long-term rescue following implantation. By shortening the timeline of cell culture, this allows for a more timely implantation and rescue from retinal degeneration, preserving a patient's vision – the ultimate goal of all vision research.

4.3.2 Understanding key dedifferentiation pathways

In addition to scaffold optimization, this work can be used as a foundation for research to elucidate key dedifferentiation pathways of the RPE cells. While SMAD3 and αSMA have already been implicated in this process, their relative importance, as well as how other pathways participate in this process has not fully been investigated. By culturing cells on low modulus scaffolds to promote dedifferentiation and then inhibiting specific pathways, the dedifferentiation of RPE cells can be understood more fully. This can be accomplished through several methods. First, while RPE cells are cultured on a low modulus scaffold, a small molecule inhibitor could be used to block a specific dedifferentiation pathway. If results indicate that dedifferentiation still occurred to the same extent as a condition in which no inhibitor was present, it could be concluded that the specific pathway being inhibited is not solely responsible for dedifferentiation. This type of study can be done with several pathways. Similar experiments can also be carried out with knock-out cells that do not contain the dedifferentiation genes. Both approaches will demonstrate the relative importance of these pathways in RPE dedifferentiation.

4.3.3 AMD Modeling

Interestingly, this study revealed significant expression of αSMA in cells cultured on low modulus scaffolds, followed by RPE detachment and loss from the scaffolds. This same phenomenon is observed in AMD. Guidry et al. demonstrated that initial changes in the RPE during AMD mimic those reported for cultured RPE cells, including αSMA expression. [82] However, during RPE atrophy αSMA-positive cells were absent suggesting that the RPE are lost rather than persisting in a dedifferentiated state. Because the cells on the low modulus scaffold behave much in the same way, further research to compare the cells in the scaffold system with native AMD affected cells to understand similarities and differences. By identifying similarities and differences in cell behavior, future researchers can optimize this system as an *in vitro* model for cell behavior in AMD and RPE atrophy.

4.3.3 Further Parameter Optimization

While this work has proven mechanical and chemical cues to be significant during RPE culture, there are several other scaffold parameters that must be taken into account in order to design a translational therapy. First, transport properties are of the utmost importance in this application. The RPE and underlying Bruch's membrane act to control much of the transport into and

out of the retina. If a scaffold-cell system is to be transplanted to replace this native function, it must be designed to mimic the transport functionality. One group in particular has done this well by using a supported sub-micron mesh scaffold that mimics the transport properties. [48]

Another major consideration of a subretinal implanted scaffold is the scaffold dimensions. A scaffold that is too thick will promote retinal detachment causing further damage to the retina. In addition to this, a scaffold that is too thin will be unmanageable for a surgeon to implant. This leaves room in the ophthalmologic field for novel implantation procedures and devices, such as the device designed by Hu et al. [83] This platform device was used to implant a 4 μm thick scaffold seeded with embryonic stem cell derived-RPE. There is still much work to be done to develop consistent successful scaffold transplantation. This dissertation was a step in that direction.

REFERENCES

1. Strauss, O., *The retinal pigment epithelium in visual function.* Physiol Rev, 2005. **85**(3): p. 845-81.
2. Curcio, C.A. and M. Johnson, *Structure, function, and pathology of Bruch's membrane.* Elastic, 2013. **146**(152): p. 210-213.
3. Bhutto, I. and G. Lutty, *Understanding age-related macular degeneration (AMD): relationships between the photoreceptor/retinal pigment epithelium/Bruch's membrane/choriocapillaris complex.* Mol Aspects Med, 2012. **33**(4): p. 295-317.
4. Center, R.I.o.t.C.T.M.D. *Age-related Macular Degeneration (AMD)*. 2009 [cited 2017 8 May]; Available from: http://www.retinaexperts.com/macular-degeneration.html.
5. Pascolini, D. and S.P. Mariotti, *Global estimates of visual impairment: 2010.* Br J Ophthalmol, 2012. **96**(5): p. 614-8.
6. Resnikoff, S., et al., *Global data on visual impairment in the year 2002.* Bull World Health Organ, 2004. **82**(11): p. 844-51.
7. Lund, R.D., et al., *Subretinal transplantation of genetically modified human cell lines attenuates loss of visual function in dystrophic rats.* Proc Natl Acad Sci U S A, 2001. **98**(17): p. 9942-7.
8. Saigo, Y., et al., *Transplantation of transduced retinal pigment epithelium in rats.* Invest Ophthalmol Vis Sci, 2004. **45**(6): p. 1996-2004.
9. Abe, T., et al., *Autologous iris pigment epithelial cell transplantation in monkey subretinal region.* Curr Eye Res, 2000. **20**(4): p. 268-75.
10. Li, L.X. and J.E. Turner, *Transplantation of retinal pigment epithelial cells to immature and adult rat hosts: short- and long-term survival characteristics.* Exp Eye Res, 1988. **47**(5): p. 771-85.
11. Arnhold, S., et al., *Adenovirally transduced bone marrow stromal cells differentiate into pigment epithelial cells and induce rescue effects in RCS rats.* Invest Ophthalmol Vis Sci, 2006. **47**(9): p. 4121-9.
12. Lopez, R., et al., *Transplanted retinal pigment epithelium modifies the retinal degeneration in the RCS rat.* Invest Ophthalmol Vis Sci, 1989. **30**(3): p. 586-8.
13. Lavail, M.M., et al., *Retinal pigment epithelial cell transplantation in RCS rats: normal metabolism in rescued photoreceptors.* Exp Eye Res, 1992. **55**(4): p. 555-62.
14. Sauve, Y., et al., *Visual field loss in RCS rats and the effect of RPE cell transplantation.* Exp Neurol, 1998. **152**(2): p. 243-50.
15. Wang, S., et al., *Grafting of ARPE-19 and Schwann cells to the subretinal space in RCS rats.* Invest Ophthalmol Vis Sci, 2005. **46**(7): p. 2552-60.
16. Lu, B., et al., *Long-term safety and function of RPE from human embryonic stem cells in preclinical models of macular degeneration.* Stem Cells, 2009. **27**(9): p. 2126-35.
17. Schwartz, S.D., et al., *Human embryonic stem cell-derived retinal pigment epithelium in patients with age-related macular degeneration and Stargardt's*

macular dystrophy: follow-up of two open-label phase 1/2 studies. Lancet, 2015. **385**(9967): p. 509-16.
18. Hynes, S.R. and E.B. Lavik, *A tissue-engineered approach towards retinal repair: scaffolds for cell transplantation to the subretinal space.* Graefes Arch Clin Exp Ophthalmol, 2010. **248**(6): p. 763-78.
19. Lu, L., M.J. Yaszemski, and A.G. Mikos, *Retinal pigment epithelium engineering using synthetic biodegradable polymers.* Biomaterials, 2001. **22**(24): p. 3345-55.
20. McHugh, K.J., S.L. Tao, and M. Saint-Geniez, *Porous poly(epsilon-caprolactone) scaffolds for retinal pigment epithelium transplantation.* Invest Ophthalmol Vis Sci, 2014. **55**(3): p. 1754-62.
21. Sugino, I.K., et al., *A method to enhance cell survival on Bruch's membrane in eyes affected by age and age-related macular degeneration.* Invest Ophthalmol Vis Sci, 2011. **52**(13): p. 9598-609.
22. Hartmann, U., F. Sistani, and U.H. Steinhorst, *Human and porcine anterior lens capsule as support for growing and grafting retinal pigment epithelium and iris pigment epithelium.* Graefes Arch Clin Exp Ophthalmol, 1999. **237**(11): p. 940-5.
23. Lee, C.J., et al., *Determination of human lens capsule permeability and its feasibility as a replacement for Bruch's membrane.* Biomaterials, 2006. **27**(8): p. 1670-8.
24. Nicolini, J., et al., *The anterior lens capsule used as support material in RPE cell-transplantation.* Acta Ophthalmol Scand, 2000. **78**(5): p. 527-31.
25. Singh, S., S. Woerly, and B.J. McLaughlin, *Natural and artificial substrates for retinal pigment epithelial monolayer transplantation.* Biomaterials, 2001. **22**(24): p. 3337-43.
26. Capeans, C., et al., *Amniotic membrane as support for human retinal pigment epithelium (RPE) cell growth.* Acta Ophthalmol Scand, 2003. **81**(3): p. 271-7.
27. Ohno-Matsui, K., et al., *The effects of amniotic membrane on retinal pigment epithelial cell differentiation.* Mol Vis, 2005. **11**: p. 1-10.
28. Singhal, S. and G.K. Vemuganti, *Primary adult human retinal pigment epithelial cell cultures on human amniotic membranes.* Indian J Ophthalmol, 2005. **53**(2): p. 109-13.
29. Stanzel, B.V., et al., *Amniotic membrane maintains the phenotype of rabbit retinal pigment epithelial cells in culture.* Exp Eye Res, 2005. **80**(1): p. 103-12.
30. Thumann, G., et al., *Descemet's membrane as membranous support in RPE/IPE transplantation.* Curr Eye Res, 1997. **16**(12): p. 1236-8.
31. Beutel, J., et al., *Inner limiting membrane as membranous support in RPE sheet-transplantation.* Graefes Arch Clin Exp Ophthalmol, 2007. **245**(10): p. 1469-73.
32. Ohno-Matsui, K., et al., *In vitro and in vivo characterization of iris pigment epithelial cells cultured on amniotic membranes.* Mol Vis, 2006. **12**: p. 1022-32.
33. Joussen, A.M., et al., *Autologous translocation of the choroid and retinal pigment epithelium in age-related macular degeneration.* Am J Ophthalmol, 2006. **142**(1): p. 17-30.

34. van Meurs, J.C., et al., *Autologous peripheral retinal pigment epithelium translocation in patients with subfoveal neovascular membranes.* Br J Ophthalmol, 2004. **88**(1): p. 110-3.
35. MacLaren, R.E., et al., *Autologous transplantation of the retinal pigment epithelium and choroid in the treatment of neovascular age-related macular degeneration.* Ophthalmology, 2007. **114**(3): p. 561-70.
36. van Zeeburg, E.J., et al., *A free retinal pigment epithelium-choroid graft in patients with exudative age-related macular degeneration: results up to 7 years.* Am J Ophthalmol, 2012. **153**(1): p. 120-7 e2.
37. Lu, J.T., et al., *Thin collagen film scaffolds for retinal epithelial cell culture.* Biomaterials, 2007. **28**(8): p. 1486-94.
38. Warnke, P.H., et al., *Primordium of an artificial Bruch's membrane made of nanofibers for engineering of retinal pigment epithelium cell monolayers.* Acta Biomater, 2013. **9**(12): p. 9414-22.
39. Farrokh-Siar, L., et al., *Cryoprecipitate: An autologous substrate for human fetal retinal pigment epithelium.* Curr Eye Res, 1999. **19**(2): p. 89-94.
40. Tezel, T.H. and L.V. Del Priore, *Reattachment to a substrate prevents apoptosis of human retinal pigment epithelium.* Graefes Arch Clin Exp Ophthalmol, 1997. **235**(1): p. 41-7.
41. Del Priore, L.V., T.H. Tezel, and H.J. Kaplan, *Survival of allogeneic porcine retinal pigment epithelial sheets after subretinal transplantation.* Invest Ophthalmol Vis Sci, 2004. **45**(3): p. 985-92.
42. Oganesian, A., et al., *A new model of retinal pigment epithelium transplantation with microspheres.* Arch Ophthalmol, 1999. **117**(9): p. 1192-200.
43. Giordano, G.G., et al., *Retinal pigment epithelium cells cultured on synthetic biodegradable polymers.* J Biomed Mater Res, 1997. **34**(1): p. 87-93.
44. Hadlock, T., et al., *Ocular cell monolayers cultured on biodegradable substrates.* Tissue Eng, 1999. **5**(3): p. 187-96.
45. Lu, L., et al., *Retinal pigment epithelial cell adhesion on novel micropatterned surfaces fabricated from synthetic biodegradable polymers.* Biomaterials, 2001. **22**(3): p. 291-7.
46. Lu, L., C.A. Garcia, and A.G. Mikos, *Retinal pigment epithelium cell culture on thin biodegradable poly(DL-lactic-co-glycolic acid) films.* J Biomater Sci Polym Ed, 1998. **9**(11): p. 1187-205.
47. Thomson, R.C., et al., *Manufacture and characterization of poly(alpha-hydroxy ester) thin films as temporary substrates for retinal pigment epithelium cells.* Biomaterials, 1996. **17**(3): p. 321-7.
48. Lu, B., et al., *Mesh-supported submicron parylene-C membranes for culturing retinal pigment epithelial cells.* Biomed Microdevices, 2012. **14**(4): p. 659-67.
49. Diniz, B., et al., *Subretinal implantation of retinal pigment epithelial cells derived from human embryonic stem cells: improved survival when implanted as a monolayer.* Invest Ophthalmol Vis Sci, 2013. **54**(7): p. 5087-96.
50. Tezcaner, A., K. Bugra, and V. Hasirci, *Retinal pigment epithelium cell culture on surface modified poly(hydroxybutyrate-co-hydroxyvalerate) thin films.* Biomaterials, 2003. **24**(25): p. 4573-83.

51. Williams, R.L., et al., *Polyurethanes as potential substrates for sub-retinal retinal pigment epithelial cell transplantation.* J Mater Sci Mater Med, 2005. **16**(12): p. 1087-92.
52. Krishna, Y., et al., *Expanded polytetrafluoroethylene as a substrate for retinal pigment epithelial cell growth and transplantation in age-related macular degeneration.* Br J Ophthalmol, 2011. **95**(4): p. 569-73.
53. Sakami, S., P. Etter, and T.A. Reh, *Activin signaling limits the competence for retinal regeneration from the pigmented epithelium.* Mech Dev, 2008. **125**(1-2): p. 106-16.
54. Steindl-Kuscher, K., et al., *Epidermal growth factor: the driving force in initiation of RPE cell proliferation.* Graefes Arch Clin Exp Ophthalmol, 2011. **249**(8): p. 1195-200.
55. Saha, K., et al., *Substrate modulus directs neural stem cell behavior.* Biophys J, 2008. **95**(9): p. 4426-38.
56. Banerjee, A., et al., *The influence of hydrogel modulus on the proliferation and differentiation of encapsulated neural stem cells.* Biomaterials, 2009. **30**(27): p. 4695-9.
57. Evans, N.D., et al., *Substrate stiffness affects early differentiation events in embryonic stem cells.* Eur Cell Mater, 2009. **18**: p. 1-13; discussion 13-4.
58. Kinnunen, K., et al., *Molecular mechanisms of retinal pigment epithelium damage and development of age-related macular degeneration.* Acta Ophthalmol, 2012. **90**(4): p. 299-309.
59. Discher, D.E., P. Janmey, and Y.-l. Wang, *Tissue Cells Feel and Respond to the Stiffness of Their Substrate.* Science, 2005. **310**(5751): p. 1139-1143.
60. Pelham, R.J. and Y.-l. Wang, *Cell locomotion and focal adhesions are regulated by substrate flexibility.* Proceedings of the National Academy of Sciences, 1997. **94**(25): p. 13661-13665.
61. Gullapalli, V.K., et al., *Impaired RPE survival on aged submacular human Bruch's membrane.* Exp Eye Res, 2005. **80**(2): p. 235-48.
62. Saika, S., et al., *Smad3 is required for dedifferentiation of retinal pigment epithelium following retinal detachment in mice.* Lab Invest, 2004. **84**(10): p. 1245-58.
63. Kuznetsova, A.V., A.M. Kurinov, and M.A. Aleksandrova, *Cell models to study regulation of cell transformation in pathologies of retinal pigment epithelium.* J Ophthalmol, 2014. **2014**: p. 801787.
64. Sheridan, C., P. Hiscott, and I. Grierson, *Retinal Pigment Epithelium Differentiation and Dedifferentiation*, in *Vitreo-retinal Surgery*, B. Kirchhof and D. Wong, Editors. 2005, Springer Berlin Heidelberg. p. 101-119.
65. Grisanti, S. and C. Guidry, *Transdifferentiation of retinal pigment epithelial cells from epithelial to mesenchymal phenotype.* Invest Ophthalmol Vis Sci, 1995. **36**(2): p. 391-405.
66. Zhu, J., *Bioactive modification of poly(ethylene glycol) hydrogels for tissue engineering.* Biomaterials, 2010. **31**(17): p. 4639-56.
67. Wang, S.Z. and R.T. Yan, *Chick retinal pigment epithelium transdifferentiation assay for proneural activities.* Methods Mol Biol, 2012. **884**: p. 201-9.

68. Haynes, J., et al., *Dynamic actin remodeling during epithelial-mesenchymal transition depends on increased moesin expression.* Mol Biol Cell, 2011. **22**(24): p. 4750-64.
69. Boochoon, K.S., et al., *The influence of substrate elastic modulus on retinal pigment epithelial cell phagocytosis.* J Biomech, 2014. **47**(12): p. 3237-40.
70. Liao, H., et al., *Influence of hydrogel mechanical properties and mesh size on vocal fold fibroblast extracellular matrix production and phenotype.* Acta Biomater, 2008. **4**(5): p. 1161-71.
71. ten Dijke, P., et al., *Characterization of type I receptors for transforming growth factor-beta and activin.* Science, 1994. **264**(5155): p. 101-4.
72. Huang, S.S. and J.S. Huang, *TGF-beta control of cell proliferation.* J Cell Biochem, 2005. **96**(3): p. 447-62.
73. Travis, M.A. and D. Sheppard, *TGF-beta activation and function in immunity.* Annu Rev Immunol, 2014. **32**: p. 51-82.
74. Fuhrmann, S., E.M. Levine, and T.A. Reh, *Extraocular mesenchyme patterns the optic vesicle during early eye development in the embryonic chick.* Development, 2000. **127**(21): p. 4599-609.
75. Idelson, M., et al., *Directed differentiation of human embryonic stem cells into functional retinal pigment epithelium cells.* Cell Stem Cell, 2009. **5**(4): p. 396-408.
76. Hotaling, N.A., et al., *Nanofiber Scaffold-Based Tissue-Engineered Retinal Pigment Epithelium to Treat Degenerative Eye Diseases.* J Ocul Pharmacol Ther, 2016. **32**(5): p. 272-85.
77. Jha, B.S. and K. Bharti, *Regenerating Retinal Pigment Epithelial Cells to Cure Blindness: A Road Towards Personalized Artificial Tissue.* Curr Stem Cell Rep, 2015. **1**(2): p. 79-91.
78. Christiansen, A.T., et al., *Subretinal implantation of electrospun, short nanowire, and smooth poly(epsilon-caprolactone) scaffolds to the subretinal space of porcine eyes.* Stem Cells Int, 2012. **2012**: p. 454295.
79. Liu, Y., et al., *Correlation of cytokine levels and microglial cell infiltration during retinal degeneration in RCS rats.* PLoS One, 2013. **8**(12): p. e82061.
80. Liu, Z., et al., *Enhancement of retinal pigment epithelial culture characteristics and subretinal space tolerance of scaffolds with 200 nm fiber topography.* Biomaterials, 2014. **35**(9): p. 2837-50.
81. Corneo, B. and S. Temple, *Sense and serendipity aid RPE generation.* Cell Stem Cell, 2009. **5**(4): p. 347-8.
82. Guidry, C., N.E. Medeiros, and C.A. Curcio, *Phenotypic variation of retinal pigment epithelium in age-related macular degeneration.* Invest Ophthalmol Vis Sci, 2002. **43**(1): p. 267-73.
83. Hu, Y., et al., *A novel approach for subretinal implantation of ultrathin substrates containing stem cell-derived retinal pigment epithelium monolayer.* Ophthalmic Res, 2012. **48**(4): p. 186-91.